AD-A138 195 PULSED GENERATION OF SINGLET DELTA OXYGEN (O2(1 DELTA)) VIA OZONE PHOTOLYSIS(U) AIR FORCE INST OF TECH WRIGHT-PATTERSON AFB OH SCHOOL OF ENGI.. L P SCHELONKA 1/1

UNCLASSIFIED DEC 83 AFIT/GEP/PH/83D-12 F/G 7/5 NL

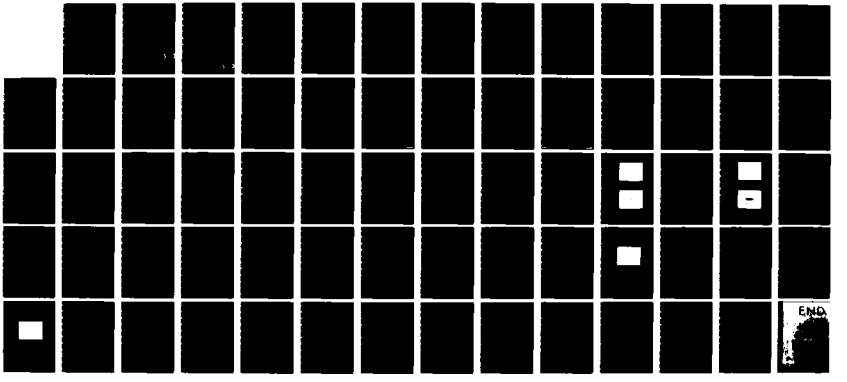

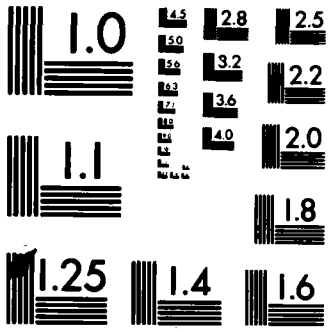

MICROCOPY RESOLUTION TEST CHART
NATIONAL BUREAU OF STANDARDS-1963-A

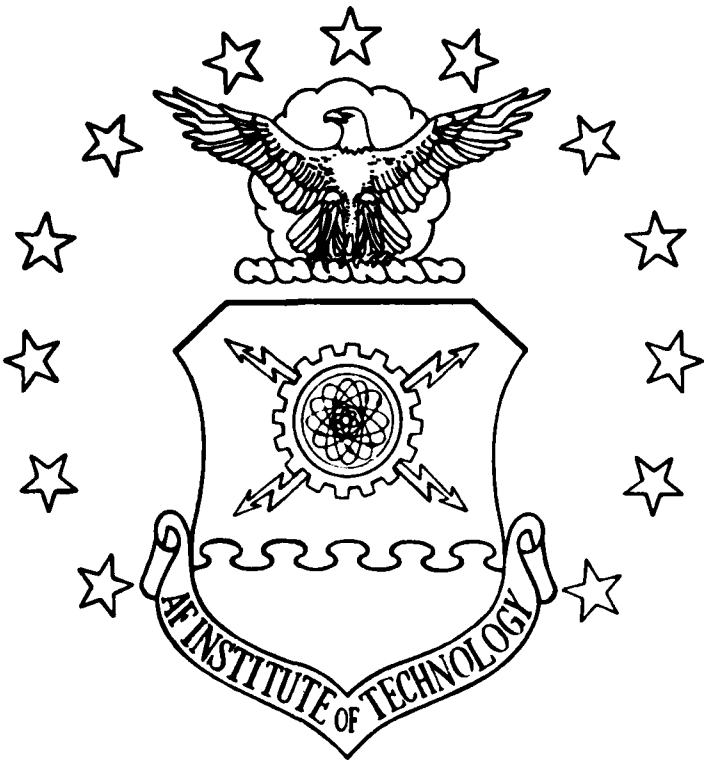

PULSED GENERATION OF SINGLET DELTA OXYGEN ($O_2(^1\Delta)$) VIA OZONE PHOTOLYSIS

THESIS

AFIT/GEP/PH/83D-12 Lee Paul Schelonka
Capt USAF

DEPARTMENT OF THE AIR FORCE
AIR UNIVERSITY
AIR FORCE INSTITUTE OF TECHNOLOGY

Wright-Patterson Air Force Base, Ohio

AFIT/GEP/PH/83D-12

PULSED GENERATION OF SINGLET DELTA OXYGEN ($O_2(^1\Delta)$) VIA OZONE PHOTOLYSIS

THESIS

AFIT/GEP/PH/83D-12 Lee Paul Schelonka
Capt USAF

AFIT/GEP/PH/83D-12

PULSED GENERATION OF SINGLET DELTA OXYGEN ($O_2(^1\Delta)$) VIA OZONE PHOTOLYSIS

THESIS

Presented to the Faculty of the School of Engineering
of the Air Force Institute of Technology
Air University
in Partial Fulfillment of the
Requirements for the Degree of
Master of Science

by

Lee Paul Schelonka, B.A.
Captain, USAF
Graduate Engineering Physics

December 1983

Acknowledgements

The author wishes to acknowledge the assistance of the following individuals at the Air Force Weapons Laboratory, Advanced Laser Branch. Dr. LaVerne Schlie provided overall direction for the experiment. 1st Lt Kerry Swift designed the ozone generating system. Mr. Robert Rathge provided day-to-day scientific assistance which was necessary to build the complicated experimental apparatus. Mr. Glen Daw helped repair and demonstrated the operation of the excimer laser. MSgt Jesse Benedict, Mr. Richard Hagenloh, and SrA Donald Stalnaker provided technician assistance throughout the experiment. The assistance of Professor Ernest A. Dorko was crucial in forming theoretical explanations for the data.

LEE PAUL SCHELONKA

Table of Contents

List of Figures

Abstract

Ozone was stored on silica gel at -77°C and photolyzed at pressures from 0.1 torr to 20 torr using an excimer laser of wavelength 2480Å. The wavelength of the emission which was detected following photolysis is in agreement with previously reported "hot band" production of $O_2(^1\Delta)_{v=1}$. Quenching of the emission occurred in 0.5 to 2 milliseconds, which may have been due to resonant transfer from $O_2(^1\Delta)$ to $I(^2P_{1/2})$. The iodine in the system was residual from prior experiments. At pressures above 3 torr, ozone combustions and detonations occurred. Combustion produced an orange glow at 5860±50Å, and detonation produced an audible shock wave which traveled at 4 ± 2 meters per second.

PULSED GENERATION OF SINGLET DELTA OXYGEN ($O_2(^1\Delta)$) VIA OZONE PHOTOLYSIS

I. Introduction

High energy chemical oxygen-iodine lasers are currently being developed by the Air Force. They depend on resonant energy transfer from excited oxygen molecules to iodine atoms. The iodine atoms, which are in an excited electronic state, transition to the ground state, giving off 1.315μ photons. The electronically excited molecular oxygen, $O_2(^1\Delta)$ is currently formed by chemical reaction of chlorine gas with a basic solution of hydrogen peroxide (Ref 1:451). This study is an investigation of the possibility of producing $O_2(^1\Delta)$ by ultraviolet laser photolysis of ozone. $O_2(^1\Delta)$ has been produced by CW photolysis of ozone using mercury lamps and ozone pressures less than 0.1 torr (Refs 2:41; 3:4323, 4324). Other experiments have reported the uv laser photolysis of ozone at pressures less than 10 millitorr (Ref 4:41). This study attempts to scale up the laser photodissociation of ozone to higher pressures.

Several reasons motivate this study of alternative $O_2(^1\Delta)$ production techniques. The current $O_2(^1\Delta)$ production method uses dangerous chemicals which present handling

difficulties. Although ozone is explosive (Ref 5:28), a safe handling technique for it has been developed (Ref 6:44,47). By-products of the current $O_2(^1\Delta)$ production method quench excited iodine (Ref 1:455). These impurities are avoided by generating $O_2(^1\Delta)$ via ozone photolysis. Finally, the chemical production of $O_2(^1\Delta)$ produces a maximum concentration of 40% $O_2(^1\Delta)$ and 60% $O_2(^3\Sigma)$, ground state oxygen (Ref 7:470). Although this fraction is sufficient to sustain lasing, alternative approaches which could produce higher $O_2(^1\Delta)$ concentrations are of interest.

The approach used in this study was to produce and photolyze ozone, and to detect radiation emitted from $O_2(^1\Delta)$, which was a product of ozone photolysis. Ozone was generated from oxygen by electric discharge in a commercial ozonator. It was purified and safely stored on silica gel at dry ice temperatures (-77°C). By raising the temperature of the silica gel, ozone was released into a photolysis cell. The ozone concentration was monitored by a pressure gauge and by absorption of ultraviolet light at a wavelength of 2537Å from a mercury lamp. An excimer laser at a wavelength of 2480Å photolyzes the ozone in pulses, producing $O_2(^1\Delta)$. The singlet delta oxygen radiatively decays to the ground state, emitting light at 6340Å and 1.27μ. This light was detected and analyzed to determine the kinetics of $O_2(^1\Delta)$ production and decay.

The organiza[illegible] as follows. A brief discussion of the theory of oxygen-iodine resonant energy transfer

provides the motivation for a discussion of the theory of $O_2(^1\Delta)$ production via ultraviolet laser photolysis of ozone. The experimental details of photolysis of O_3 and detection of $O_2(^1\Delta)$ emission are then described. Finally, the results of the photolytic production of $O_2(^1\Delta)$ are given along with recommendations for further study.

II. Theory

The following energy transfer scheme for oxygen-iodine systems has been reported (Ref 7:469):

$$O_2(^1\Delta) + O_2(^1\Delta) \rightarrow O_2(^1\Sigma) + O_2(^3\Sigma) \quad (1)$$

$$O_2(^1\Sigma) + I_2 \rightarrow O_2(^3\Sigma) + 2I(^2P_{3/2}) \quad (2)$$

$$O_2(^1\Delta) + I(^2P_{3/2}) \rightleftarrows O_2(^3\Sigma) + I^*(^2P_{1/2}) \quad (3)$$

$$I^*(^2P_{1/2}) + O_2(^1\Delta) \rightarrow O_2(^1\Sigma) + I(^2P_{3/2}) \quad (4)$$

$$I^*(^2P_{1/2}) \rightarrow I(^2P_{3/2}) + h\nu \quad (\lambda=1.315\mu) \quad (5)$$

Molecular iodine is dissociated by excited molecular oxygen. Oxygen in the singlet delta state excites atomic iodine from its ground state into an excited spin-orbit state $I^*(^2P_{1/2})$. This excited state radiatively decays to provide laser photons of wavelength 1.315μ. Figure 1 is an energy level diagram of the oxygen and iodine states in this system (Ref 8:560). $O_2(^1\Delta)$ and $I^*(^2P_{1/2})$ lie at nearly the same energy above the ground state: approximately 8000 cm^{-1}. The I* energy level is slightly below that of $O_2(^1\Delta)$, decreasing the activation energy and increasing the rate constant for resonant energy transfer. The rate constant for reaction (3) is 7.6×10^{-11} cm^3 $molecule^{-1}$ sec^{-1} (Ref 1:451). The presence of I_2 in the system can quench I* quickly, so it is important that reaction (4) produces $O_2(^1\Sigma)$, which dissociates I_2. The energy level diagram in Figure 1 shows that $O_2(^1\Sigma)$ lies at an energy just above the dissociation

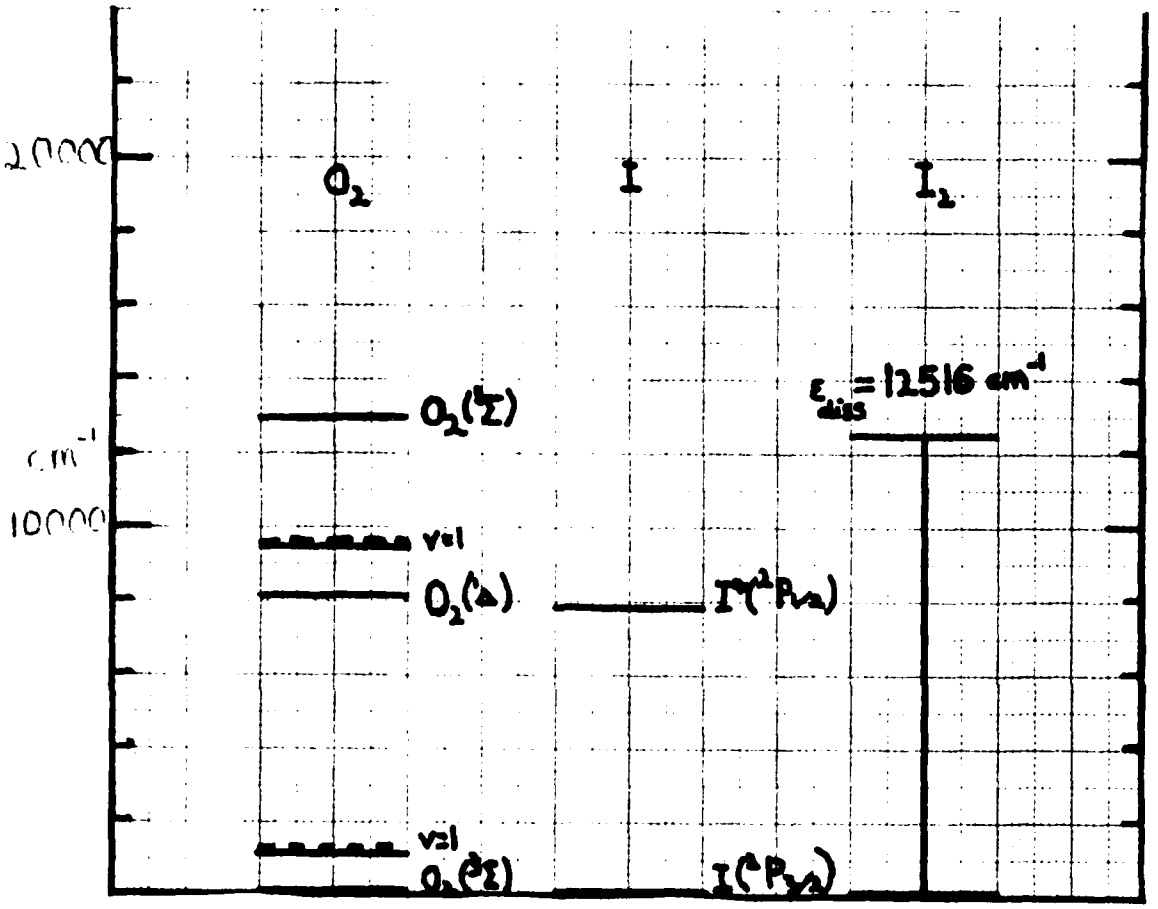

Figure 1. Energy Level Diagram of Oxygen-Iodine System

energy of I_2, providing an efficient I_2 dissociation mechanism (Ref 2:9).

The minimum fraction of excited oxygen which will support a population inversion is 17% $O_2(^1\Delta)$ and 83% $O_2(^3\Sigma)$ (Ref 7:469). Since the rates and equilibrium points of reactions (1), (3), and (4) are proportional to the concentration of $O_2(^1\Delta)$, increasing the concentration of $O_2(^1\Delta)$ makes the process faster and more complete. Thus a photolytic generator of $O_2(^1\Delta)$ will produce an oxygen-iodine laser with more available power if it produces a greater fraction of $O_2(^1\Delta)$ than the current chemical process does. The current chemical process involves bubbling chlorine gas through a basic solution of hydrogen peroxide:

$$Cl_2 + H_2O_2 + 2NaOH \rightarrow O_2(^1\Delta) + 2H_2O + 2NaCl \qquad (6)$$

This reaction typically produces only 40% $O_2(^1\Delta)$ and 60% $O_2(^3\Sigma)$ (Ref 7:469).

Since the presence of ground state oxygen $O_2(^3\Sigma)$ limits the efficiency of oxygen-iodine lasers, the fraction of $O_2(^1\Delta)$ compared to ground state oxygen should be as high as possible. In the ultraviolet photolysis of ozone, three states of O_2 are produced (Ref 1:452):

$$O_3 + h\nu\ (\lambda<3000\text{Å}) \rightleftharpoons \begin{cases} O_2(^1\Sigma) + O(^1D) \\ O_2(^1\Delta) + O(^1D) \\ O_2(^3\Sigma) + O(^3P) \end{cases} \qquad (7)$$

Approximately 90% $O_2(^1\Delta)$ is produced in reaction 7(b) with 10% $O_2(^3\Sigma)$ produced in reaction 7(c) (Ref 9:1402). Since ozone is an efficient quencher of $O_2(^1\Sigma)$ (Ref 1:455) the concentration of $O_2(^1\Sigma)$ is small. The photolytic generator of $O_2(^1\Delta)$ has the potential to double the efficiency of current $O_2(^1\Delta)$ generators.

In a photolysis experiment, the rate of ozone dissociation is proportional to the intensity of incident radiation (Ref 1:452), and is given by:

$$\nu_D = \frac{I}{h\nu} \cdot \sigma_d \qquad (8)$$

where ν_D is the dissociation rate in sec^{-1}

I is the intensity of watts/cm^2

σ_d is the ozone photolysis cross section

ν is the frequency of incident radiation

In this case, the peak laser pulse intensity was 6.8 MW/cm^2, the wavelength was 2480Å, and the cross section was 6×10^{-18} cm^2 (Ref 1:452). If I is assumed to be constant (as a first approximation) throughout the photolysis region, then ν_D is 5.9×10^7 sec^{-1}. The rate equation for ozone dissociation is:

$$\frac{d[O_3]}{dt} = \nu_D [O_3] \qquad (9)$$

so

$$[O_3] = [O_3]_0 \, e^{-\nu_D t} \tag{10}$$

Thus the characteristic time τ_D for exponential ozone decay is $1/\nu_D$ or 16.9 nanoseconds. Since the laser pulsewidth was 16 ns, the concentration of ozone is expected to decline to 39% of its pre-pulse value.

The intensity of radiation decreases as the laser pulse penetrates deeper into the ozone, according to the Beer-Lambert law (Ref 10:857). Since ozone in the cell experiences attenuated radiation, the rate of ozone dissociation is reduced. The appendix provides a sample calculation of the amount of ozone dissociated when 1 torr of ozone is initially present.

Quenching of $O_2(^1\Delta)$ takes place according to the following reaction scheme:

$$O_2(^1\Delta) + M \xrightarrow{k_M} O_2(^3\Sigma) + M \tag{11}$$

where M is a chemically inert species.

This reaction reduces the amount of $O_2(^1\Delta)$ according to the rate equation:

$$\frac{d[O_2(^1\Delta)]}{dt} = -k_M \, [O_2(^1\Delta)] \, [M] \tag{12}$$

If [M] is constant, the decay is exponential:

$$[O_2(^1\Delta)] = [O_2(^1\Delta)]_0 e^{-k_M[M]t} \tag{13}$$

The characteristic time for quenching, τ_q, is given by:

$$\tau_q = \frac{1}{k\ [M]} \tag{14}$$

Table 1 lists quenching agents, rate constants, and anticipated concentrations of agents.

TABLE I

QUENCHING AGENTS AND THEIR RATE CONSTANTS

Quenching Agent-M	[M] (cm^{-3})	K_M	Reference
O	10^{15}-10^{17}	$4 \times 10^{-15} cm^3/sec$	11:149
$O_2(^1\Delta)$	10^{13}-10^{15}	$2 \times 10^{-18} cm^3/sec$	12:93
Helium	10^{15}-10^{17}	$8 \times 10^{-21} cm^3/sec$	11:149
Helium impurities (H2, CO)	10^{11}-10^{13}	$7 \times 10^{-17} cm^3/sec$	11:149
Wall		$.01\ sec^{-1}$	12:95

Ozone is by far the most efficient quencher of $O_2(^1\Delta)$ in this group of anticipated agents. The appendix provides sample calculations of the quenching of $O_2(^1\Delta)$ produced by 1 torr of ozone. If 1 torr of ozone is initially present, 0.45 torr dissociates and 0.55 torr of ozone remains to quench $O_2(^1\Delta)$. This quenching occurs with a characteristic time of 13 m sec. Other projected quenching agents quench two orders of magnitude slower.

$O_2(^1\Delta)$ decays by emission to the ground state in two

ways (Ref 2:27). The most intense emission at pressures less than 100 torr occurs in the infrared:

$$O_2(^1\Delta) \rightarrow O_2(^3\Sigma) + h\nu \quad (\lambda = 1.27\mu) \tag{15}$$

This emission has a radiative lifetime τ_r of 3660 seconds. The number of $O_2(^1\Delta)$ molecules emitting at 1.27μ from reaction (15) is given by:

$$N(t) = N_0 - n(t) \tag{16}$$

where N_0 is the initial number of $O_2(^1\Delta)$ molecules

n is the number of $(O_2{}^1\Delta)$ molecules remaining

But n(t) is governed by exponential decay:

$$n(t) = N_0 e^{-t/\tau_r} \tag{17}$$

After 1 second (t=1) the number of $O_2(^1\Delta)$ molecules is:

$$n(1) = N_0 e^{-1/\tau_r} \tag{18}$$

and

$$N(1) = N_0(1-e^{-1/\tau_r}) \tag{19}$$

Since $\tau_r >> 1$ second,

$$N(1) \simeq \frac{N_0}{\tau_r} \tag{20}$$

The appendix provides a sample calculation of the amount of light emitted from $O_2(^1\Delta)$ produced by 1 torr of ozone.

The second emission process is a cooperative energy pooling process, in which the energy from two $O_2(^1\Delta)$ molecules produces a single photon (Ref 13:658):

$$O_2(^1\Delta) + O_2(^1\Delta) \rightarrow O_2(^3\Sigma) + O_2(^3\Sigma) + h\nu \quad (\lambda=6340\text{Å}) \quad (21)$$

Since the process depends on collisions, its rate is proportional to the square of the concentration of $O_2(^1\Delta)$. The rate constant for reaction (21) is 3×10^{-23} cm^3 sec^{-1} (Ref 2:27). In the appendix, a sample calculation of the amount of light at 6340Å produced in reaction (21) is given. At concentrations near 1 torr the power of 1.27μ radiation is much higher than that for 6340Å radiation.

In summary, several important conclusions can be drawn from the ozone photolysis theory. Ozone photolysis offers potentially higher concentrations of $O_2(^1\Delta)$ than the widely used chemical method. Dissociation of ozone occurs with a characteristic time approximately equal to the laser pulsewidth, so approximately 45% of the ozone dissociates. The fastest anticipated quenching process, ozone quenching, takes several milliseconds when the initial ozone pressure is 1 torr. Finally, the theory predicts that much more light is produced at 1.27μ than at 6340Å.

III. Experimental Details

This section discusses the apparatus and techniques used to produce, purify, and photolyze ozone safely. Then it describes the apparatus and techniques used to detect emission from $O_2(^1\Delta)$ produced by ozone photolysis. Finally, the ultraviolet absorption system used to monitor ozone concentration is discussed.

To produce ozone safely, the potential for combustion and detonation must be controlled. Self combustion of pure ozone to molecular oxygen occurs by the following reaction (Ref 14:38):

$$O_3 \rightarrow 3/2\ O_2 + 33.9\ \text{kcal(mole)}^{-1} \tag{22}$$

A possible mechanism for the reaction is:

$$O_3 \rightarrow O_2 + O\cdot \tag{23}$$

$$O\cdot + O\cdot \rightarrow O_2 \tag{24}$$

Combustion is self-sustaining when collisions occur to break down the ozone. For example, an oxygen atom with translational energy greater than the activation energy for ozone dissociation may collide with an ozone molecule, producing another oxygen atom and an oxygen molecule:

$$O\cdot + O_3 \xrightarrow{k_{25}} O_2 + O\cdot + O\cdot \tag{25}$$

$$O\cdot + O\cdot \xrightarrow{k_{26}} O_2 \qquad (26)$$

Also, an oxygen molecule with translational energy greater than the activation energy for ozone dissociation may collide with an ozone molecule, producing another oxygen molecule and an oxygen atom:

$$O_2 + O_3 \xrightarrow{k_{27}} O_2 + O_2 + O\cdot \qquad (27)$$

$$O\cdot + O\cdot \xrightarrow{k_{28}} O_2 \qquad (28)$$

The criteria for self-sustaining combustion is that, on the average, each oxygen atom or molecule dissociates one ozone molecule. This can happen if k_{25} is greater than k_{26}, or k_{27} is greater than k_{28}; while at the same time the products of reaction (25) or (27) have translational energy greater than the activation energy for ozone dissociation. If these conditions hold, a steady state chain reaction takes place to sustain combustion. If k_{25} is much greater than k_{26} or if k_{27} is much greater than k_{28} then detonation may occur. The criteria for detonation is that, on the average, each oxygen atom or molecule dissociates two or more ozone molecules. This leads to exponential growth of the number of oxygen atoms and molecules, rapid dissociation of ozone, and production of a shock wave. Combustion and mild,

nondestructive detonations occurred when the pressure of ozone undergoing photolysis exceeded 3 torr. At atmospheric pressures, ozone detonates violently (Ref 5:28). However, ozone adsorbed onto silica gel at dry ice temperature (-77°C) has a low enough vapor pressure to prohibit detonation, even when iron wires embedded in the silica gel are ignited by electric currents (Ref 6:47).

The ozone production and purification system was prepared as follows. Referring to Figure 2, the silica gel and the molecular sieve were baked out under vacuum using an oil bath at 120°C for 12 hours to remove residual water vapor and ozone from prior experiments. Approximately 2 kg of silica gel was used in a 3 liter trap, and approximately 0.5 kg of molecular sieve was used in a 0.5 liter trap. Following bakeout, the system was pumped down with a Welch Duo-Seal Model 1397 vacuum pump to less than 100 microns (the limit of measurement of the Veeco DU-4AM thermocouple and the Veeco TG-270 gauge monitor). When the pump was isolated from the vacuum system to check the outgas rate, the pressure declined. Apparently the silica gel and the molecular sieve absorbed residual gases as they cooled. All tubing was either stainless steel or polyethylene to prevent ozone corrosion. The connections were all leak checked under vacuum with acetone. Finally, a dry ice-trichloroethylene cold bath at -77°C was placed around the silica gel trap to cool the silica gel so ozone would adsorb onto it.

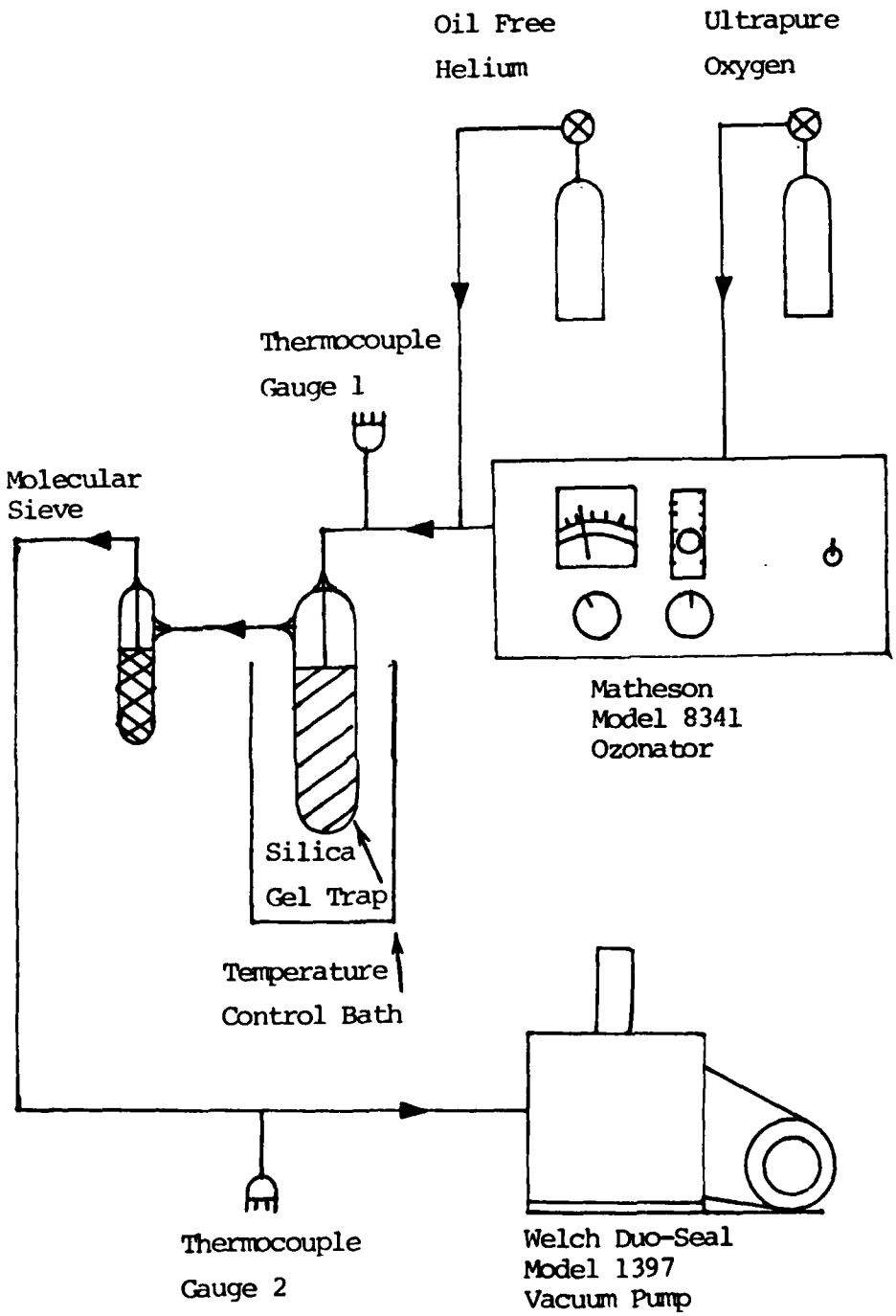

Figure 2. Ozone Production Apparatus

Ultrapure (99.98%) oxygen was used for ozone formation because impurities react quickly with ozone and decrease the production rate. The oxygen flowed at 10-15 p.s.i., as measured by the oxygen regulator gauge, into the Matheson Model 8341 ozonator, whose listed pressure limit is 20 p.s.i. gauge pressure. The O_2 flow rate in the ozonator was adjusted by a valve on its front panel to be 8 to 10 liters per minute. The power setting on the ozonator's electric discharge was then brought up to 100-150 watts. According to the manual, this produces a mixture of 2%-3% ozone and 97%-98% unexcited oxygen. The ozone-oxygen mixture then flowed through the silica gel at $-77^{o}C$. At dry ice temperatures, ozone is adsorbed onto the silica gel, causing a purplish blue color on the gel, while oxygen flows through with negligible adsorption (Ref 6:46). Up to 10% by weight of ozone can be stored on silica gel at dry ice temperatures. After 1-2 hours of production and adsorption, the ozonator was turned off and purged with oxygen, which was vented out of the building. After purging, the vent was closed and the system was pumped down to 0.2-0.5 torr. A small amount of helium was flowed to purge the lines of oxygen and reduce the concentration of ozone entering the vacuum pump. Vacuum pump oil reacts strongly with ozone and oxygen at 1 atmosphere. At pressures less than 20 torr, it is not necessary to dilute the ozone to operate the vacuum pump safely because the molecular sieve decomposed the ozone before it entered the vacuum pump.

Pure ozone was pumped through the apparatus by switching the vacuum flow using valves. Figure 3 shows the layout of the valves in the apparatus. Valve 3 was opened with valve 2 closed to evacuate the apparatus. Then valve 2 was opened and valve 1 was closed, directing ozone flow through the test cell. The pressure of ozone was controlled by changing the temperature of the bath surrouding the silica gel trap. At dry ice temperatures, equilibrium occurred for ozone adsorbed on the silica gel and free ozone at a vapor pressure of approximately 1 torr. Because of this equilibrium, pure ozone at 1 torr could be flowed through the system when the silica gel was at -77°C. To achieve higher pressures, the temperature of the silica gel was increased. By removing the cold bath the pressure was increased to 3 torr. The highest production pressures, in excess of 20 torr, were produced when an oil bath at room temperature was placed around the silica gel trap. Pressures below 1 torr were achieved by closing valve 2, which blocked ozone flow to the photolysis and absorption cells. The pressure declined from 1 torr to less tha 0.1 torr over several minutes, so multiple measurements at different pressures were taken as the pressure declined.

The four-port photolysis cell was designed to permit detection of $O_2(^1\Delta)$ emission at right angles to the incident laser radiation. Figure 4 shows a cross section of the photolysis cell and the detection apparatus. A KrF excimer laser provided 16 nanosecond pulses with 250 mJ of 2480Å

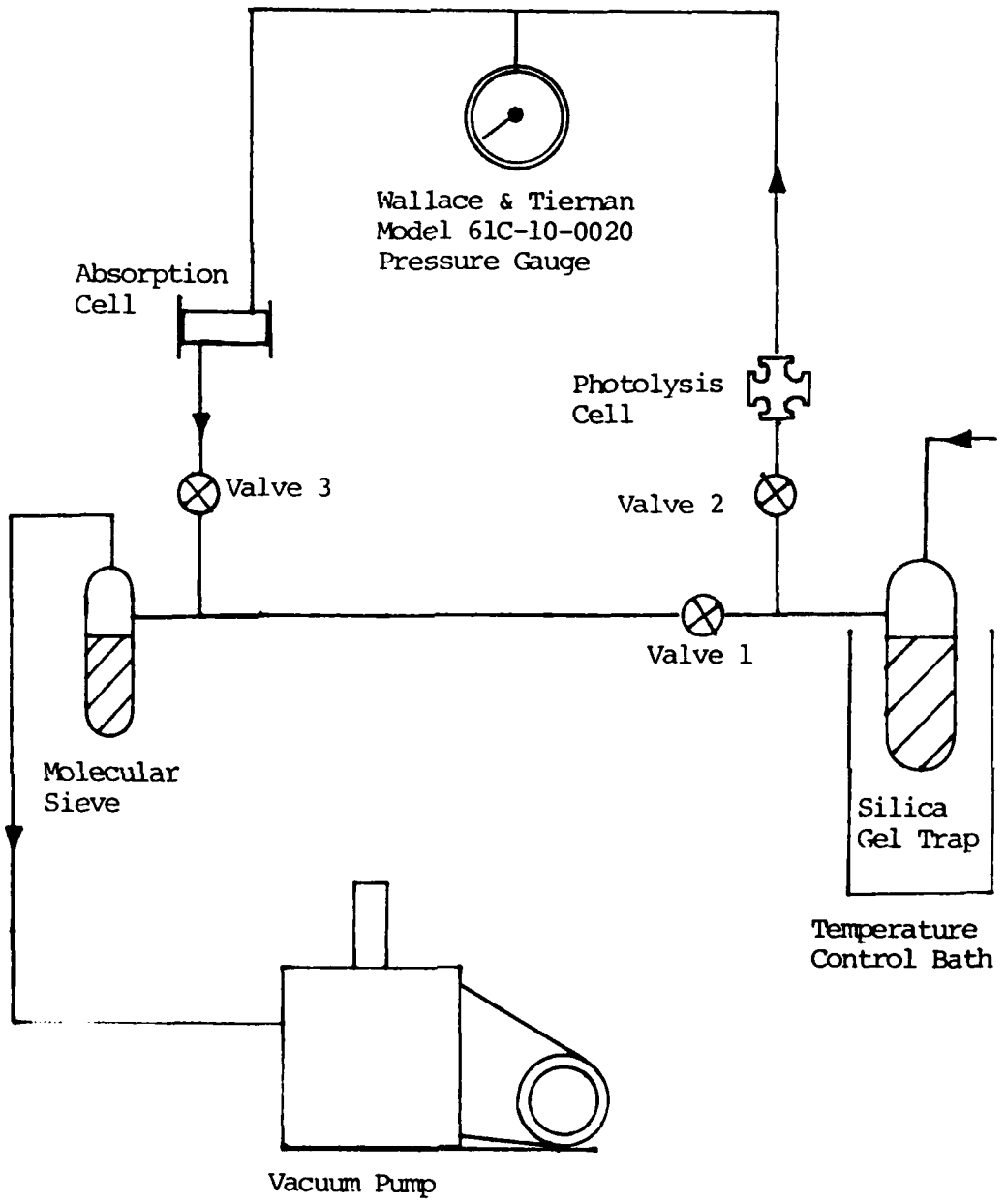

Figure 3. Experimental Apparatus (Valve Layout)

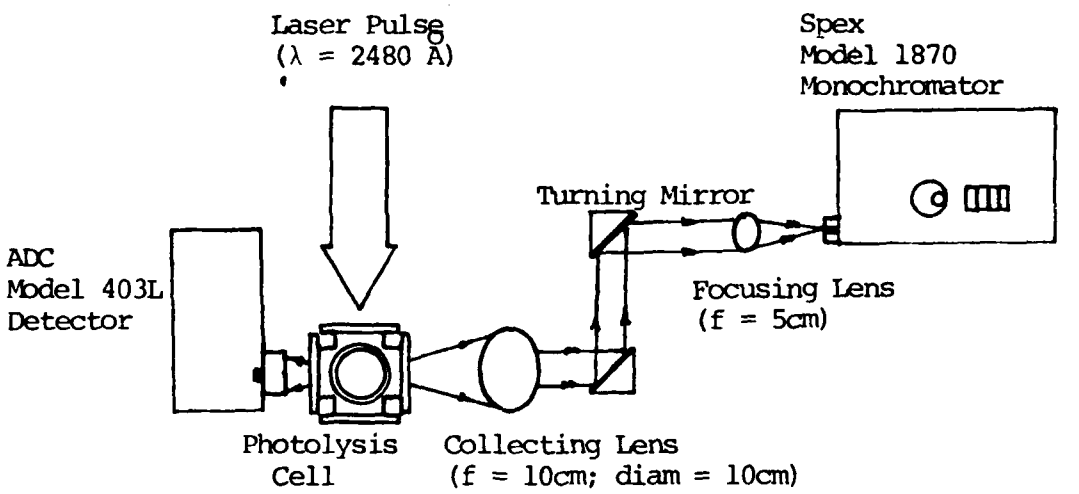

Figure 4: Photolysis/Detection Layout

radiation. The windows on the photolysis cell were 2.5 cm diameter, 0.2 cm thick quartz, possessing transmissivities of greater than 70% for 2480Å radiation and greater than 90% for 1.27μ radiation. The Applied Detector Corporation model 403 L intrinsic germanium detector responsivity is given in Figure 5. At 1.27μ, the responsivity is approximately 10^{10} volts per watt. Its Noise Equivalent Power is (1.36, 10-500, 1) 10^{-15} W $Hz^{-1/2}$ (Ref 13:1-4). The detector was biased to -250 V. Its 0.25 cm^2 active area intercepts a solid angle of 2.2×10^{-3} steradians measured from the center of the photolysis cell. Based on these data, a 1 volt output from the detector would correspond to 4.5×10^{-8} watts produced at the photolysis cell. A 1.27μ center frequency, 70Å FWHM interference filter with a peak transmissivity of 57% was used with the detector to pass only the $O_2(^1\Delta)$ emission. Signals were displayed on the Tektronix 7633 oscilloscope and recorded using a scope camera.

To monitor 6340Å emission a Spex Model 1870 half meter monochromator with variable slits was used. Spectrographs were taken using slit widths from 100μ to 1 mm with 2400 g/mm and 1200 g/mm holographic gratings. Polaroid type 57, ASA 3000 film was used to pick up faint light. An RCA C31034 photomultiplier tube was also used with the monochromator. Its photocathode response, given as trace 128 in Figure 6, is approximately 60 milliamps per watt from 4000Å to 8500Å. The gain of the photomultiplier was

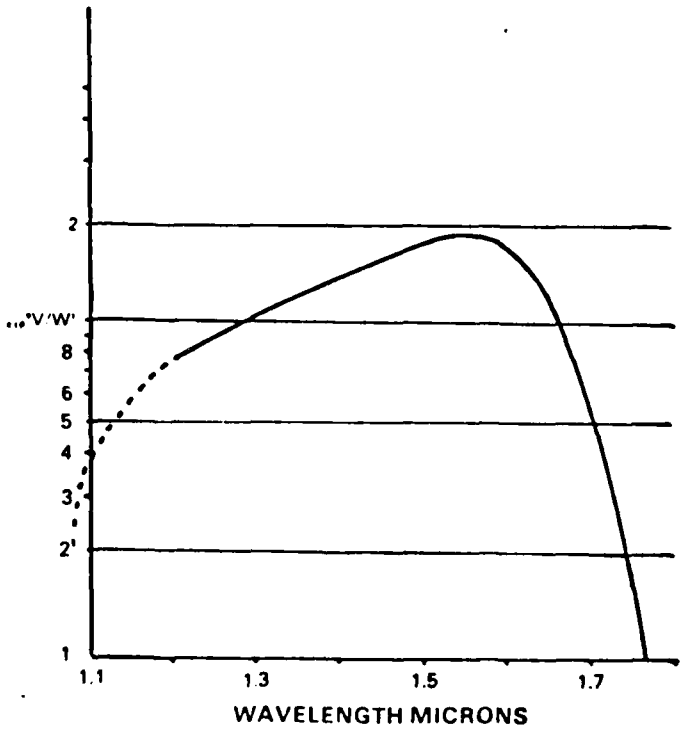

Figure 5. ADC Model 403L Detector Responsivity vs Wavelength

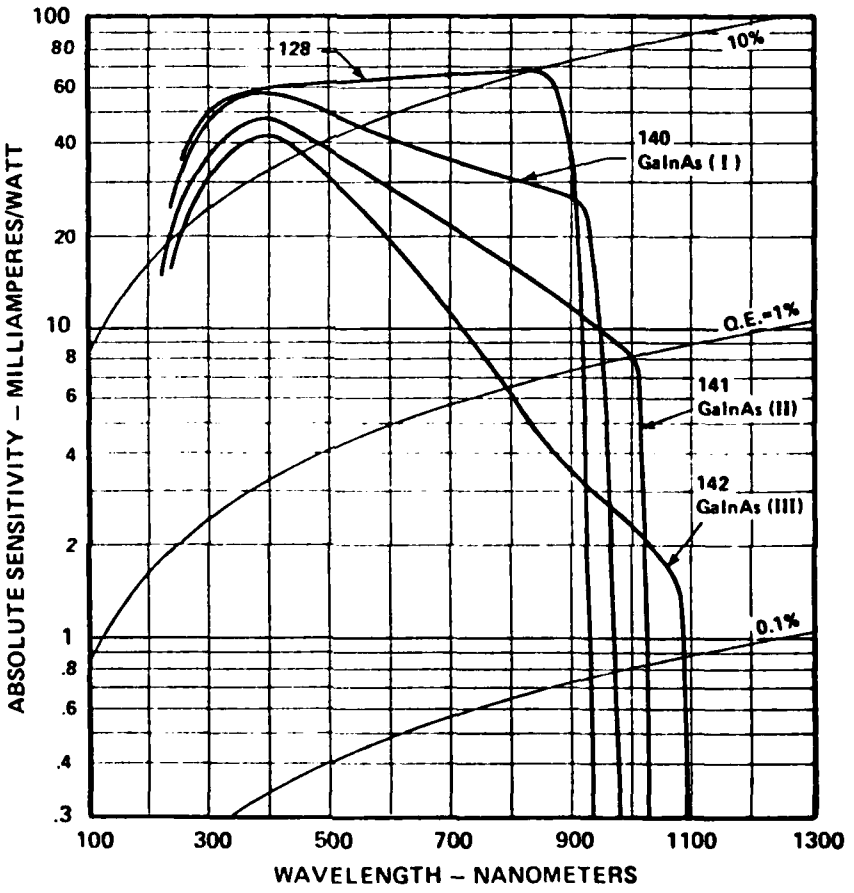

Figure 6. RCA Photocathode Responsivity vs Wavelength

6×10^5 when biased to 1500 volts. The entrance slit subtended a solid angle of 2.3×10^{-4} steradians when imaged into the space of the photolysis cell. Output from the PMT was amplified with a 1 megohm impedance oscilloscope amplifier. These conditions imply that a 1 volt signal corresponds to 1.06×10^{-7} watts at the photolysis cell. From the appendix, 1 torr of ozone dissociates to form $O_2(^1\Delta)$ which gives off 1.8×10^{-9} watts at 6340Å. This corresponds to a signal of 17 millivolts from the PMT system.

Two methods were used to measure the pressure of ozone. A Wallace and Tiernan model 61C-10-0020 pressure gauge directly measured the total pressure of all gases present, from 0.1 torr to 20 torr. In addition, an ultraviolet absorption system was used to monitor the pressure of ozone alone. Figure 7 shows the layout of the absorption experiment. Light from the Spectroline mercury lamp was collected by a lens and chopped at 30 Hz. Then it passed through an iris of diameter 0.7 cm into the 5 cm long, 1 cm diameter absorption cell. Ultraviolet light of wavelength 2537Å is absorbed by ozone according to the Lambert-Beer law with an absorption coefficient of 131 $cm^{-1} atm^{-1}$ (Ref 10:857). The pressure of ozone can be determined from the amount of absorption. The attenuated light emerging from the absorption cell was focused onto the 100μ entrance slit of a Jarrell Ash 0.25 meter monochromator with a grating having 2365 lines per millimeter blazed at 3000Å. The

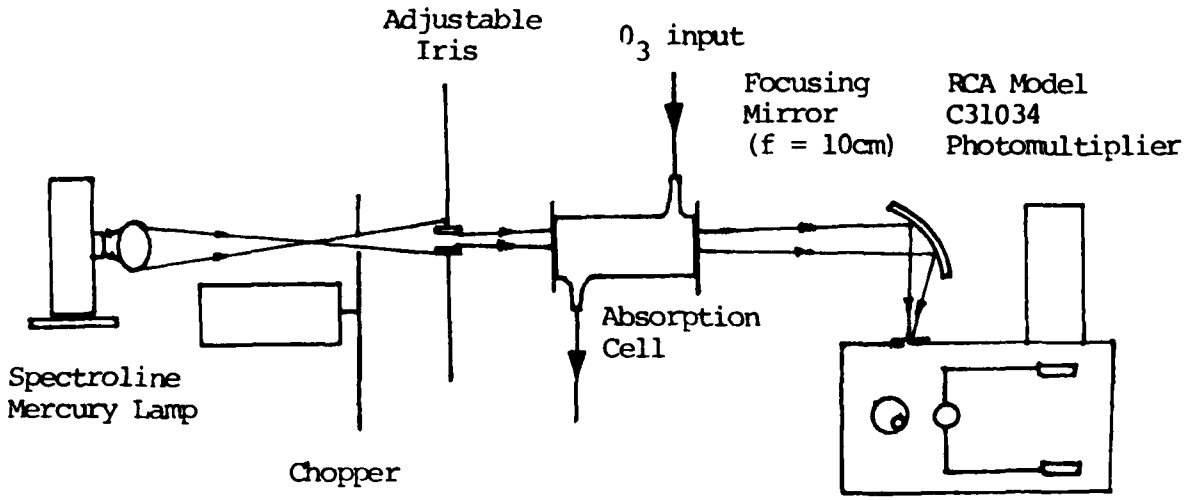

Figure 7. Absorption Measurement Layout

dispersed light passed through a 100μ exit slit to an RCA C31034 photomultiplier tube. In Figure 6, the PMT response to 2500Å light is down by only a factor of 1/2 from its peak, so the C31034 PMT is able to monitor 2500Å light accurately. A Princeton Applied Research Model 121 lock-in amplifier demodulated the light, and the signal was recorded on a HP 7100 strip chart recorder.

When the pressure of ozone was between 0.1 torr and 5 torr, both the pressure gauge and the absorption system were used. In this pressure range, the two devices agreed to better than 20%. Above 5 torr, over 99% of the light was absorbed, and the strip chart record was so close to zero that it was unusable. The pressure gauge was used exclusively at these high pressures. Below 0.1 torr the pressure gauge was off scale so absorption was used exclusively. During photolysis, the total pressure as measured by the gauge rose slightly due to an increased number of moles of gas present (one mole of ozone producing one and one-half moles of oxygen). At the same time, the absorption system indicated a reduction in ozone pressure during photolysis.

By monitoring absorption before, during, and after photolysis, the fraction of ozone photolyzed was determined. Figure 8 is a portion of the strip chart record monitoring absorption, from which ozone pressure is calculated. The chart time scale is 1.25 cm per minute, the top of the grid is 100% absorption, and the bottom line is 0% absorption.

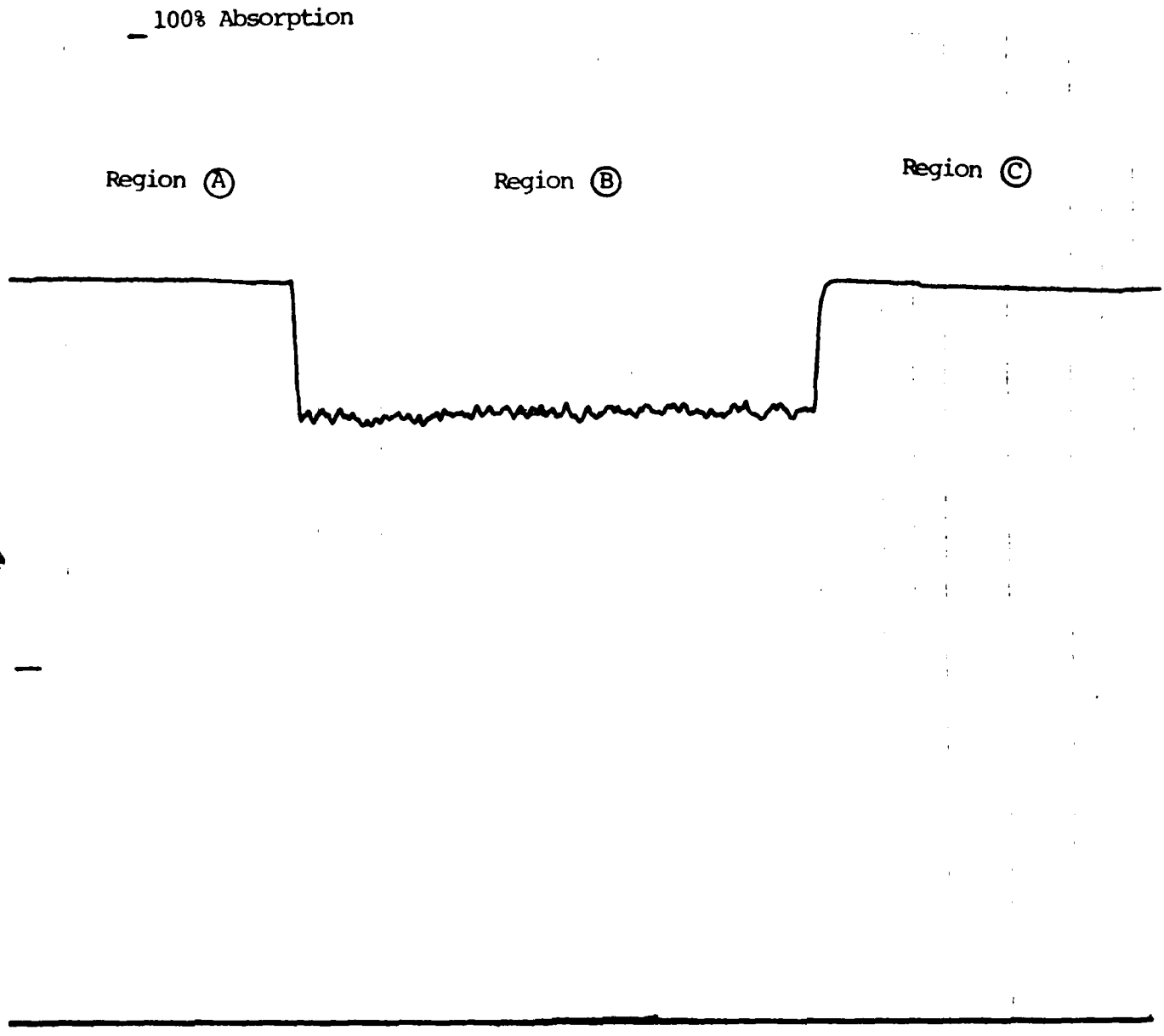

Figure 8. Change in Absorption During Photolysis

In region A, when the laser was blocked and no photolysis took place, the ozone pressure was steady at 1.67±0.03 torr. In region B, the laser was photolyzing the ozone at 1.5 pulses per second, and the pressure was 1.13±0.06 torr. Finally, in region C, the laser was blocked again and the pressure stabilized at 1.65±.04 torr. This shows that the ozone flow rate can be adjusted to give a steady pressure over a ten minute period, and that steady photolysis of 30% of the ozone occurs when the laser pulses at 1.5 Hz.

In summary, ultrapure oxygen flowed through an ozonator to produce ozone at up to 3% concentration. The ozone was adsorbed onto silica gel at -77°C for safe storage. Ozone was removed at pressures ranging from 0.1 torr to over 20 torr by raising the temperature of the silica gel, and was photolyzed by an excimer laser at a wavelength of 2480Å. $O_2(^1\Delta)$ produced by photolysis emitted radiation which was detected by an intrinsic germainium detector and a photomultiplier tube. The pressure of ozone was monitored by an ultraviolet absorption system and a pressure gauge.

IV. Results and Discussion

This section presents data from the detector systems monitoring $O_2(^1\Delta)$ emission at initial ozone pressures less than 3 torr. The quenching of emission was much faster than quenching by residual ozone would explain. This may have been due to quenching by residual iodine, which was known to be present in the system. The section also presents data on ozone combustions and detonations, which indicate chain reactions for combustion and the presence of a shock wave during detonation. During combustion, a doublet at 5860 ± 50Å was the only feature observed in the visible spectrum. This may have been caused by cooperative emission of $O_2(^1\Delta)_{v=1}$ with $O_2(^1\Delta)_{v=0}$.

Detection of $O_2(^1\Delta)$ Radiation

To determine the noise level of the 1.27μ detector system, data was taken with the laser irradiating the photolysis cell but with no ozone present. The oscilloscope was triggered with a synchronous pulse from the laser, and photographs were taken of the stored traces. The trace was positioned so that its leading edge was clearly visible. Figure 9 shows the noise level with no photolysis is 1.5 millivolts. Radio frequency interference from the laser, which would show up as a narrow spike on the leading edge of the trace, is not seen above the noise level. Figure 9 also shows that cell phosphorescence is negligible at 1.27μ.

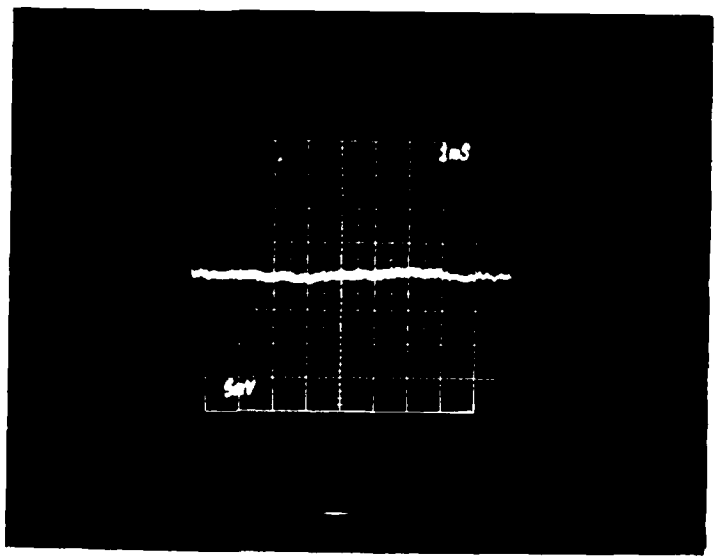

Figure 9. Detector Response: No Ozone Present

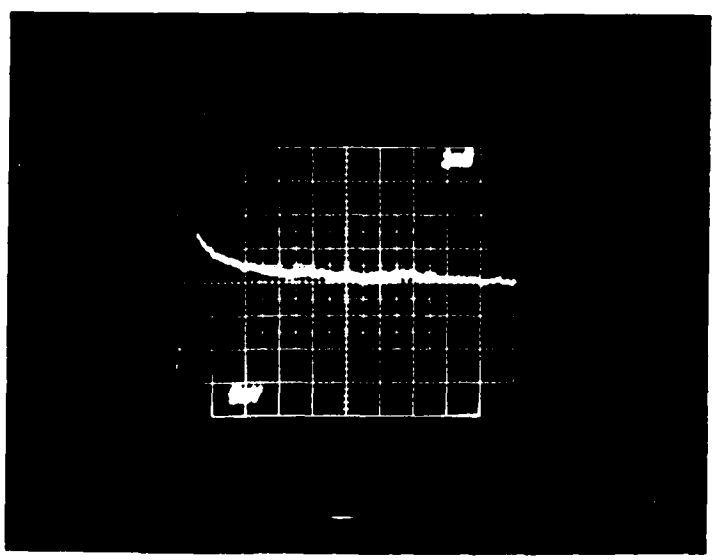

Figure 10. Detector Response: 0.35 torr Ozone

TABLE II

Measured Decay Times and Theoretical Quench Times for Initial Ozone Pressures From 0.1 Torr to 3 Torr

Initial Ozone Pressure (torr)	Observed Decay Time (ms)	Predicted Decay Time (ms)
0.01	0.5±.2	1300
0.014	0.6±.2	928
0.04	0.5±.2	325
0.05	0.5±.1	260
0.05	0.6±.2	260
0.12	1.2±.2	108
0.35	1.5±.2	37
1.0	1.6±.4	13
1.0	2.0±.2	13
1.1	1.5±.2	12
1.3	1.8±.5	10
1.5	1.8±.1	8.7
2.2	2.0±.2	5.9
2.8	2.0±.4	4.6

Oscillographs were taken at several ozone pressures during photolysis to measure the emission from $O_2(^1\Delta)$. Figure 10 shows the detector's output when 0.35 torr of ozone was photolyzed Figures 11 and 12 show the detector output for 1 torr and 2.8 torr. By plotting the logarithm of the amplitude versus time for the data at 1 torr and 2.8 torr, straight lines resulted (Figures 13 and 14). The exponential decay time constants are the reciprocals of the slopes of these lines. Table 2 presents the measured decay constants below 3 torr along with the decay times predicted in equation (14) for the reaction:

$$O_2(^1\Delta) + O_3 \rightarrow O_2(^3\Sigma) + O_3 \qquad (29)$$

The observed decay times are shorter than those predicted by

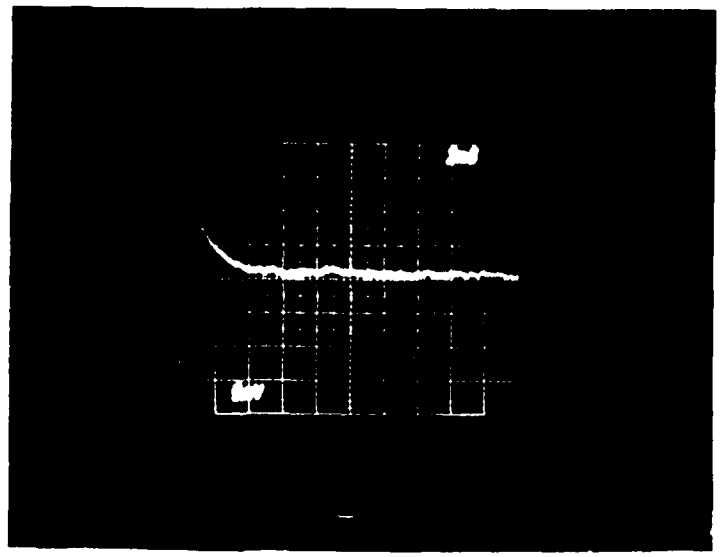

Figure 11. Detector Response: 1 torr Ozone

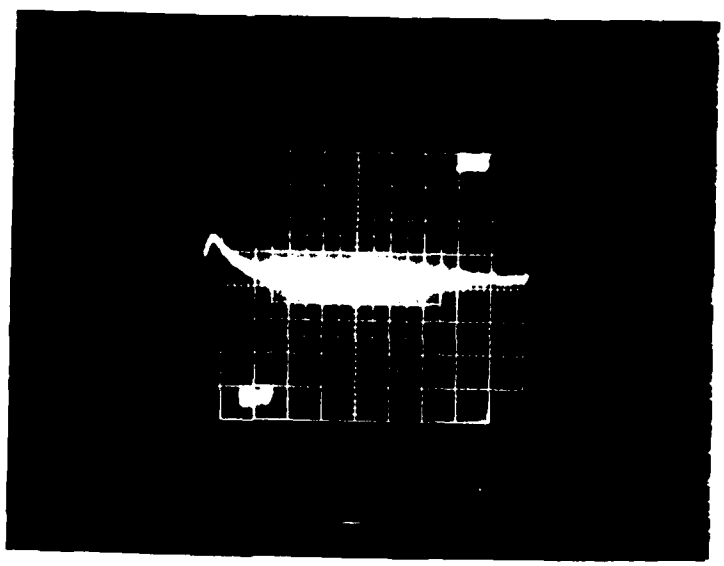

Figure 12. Detector Response: 2.8 torr Ozone

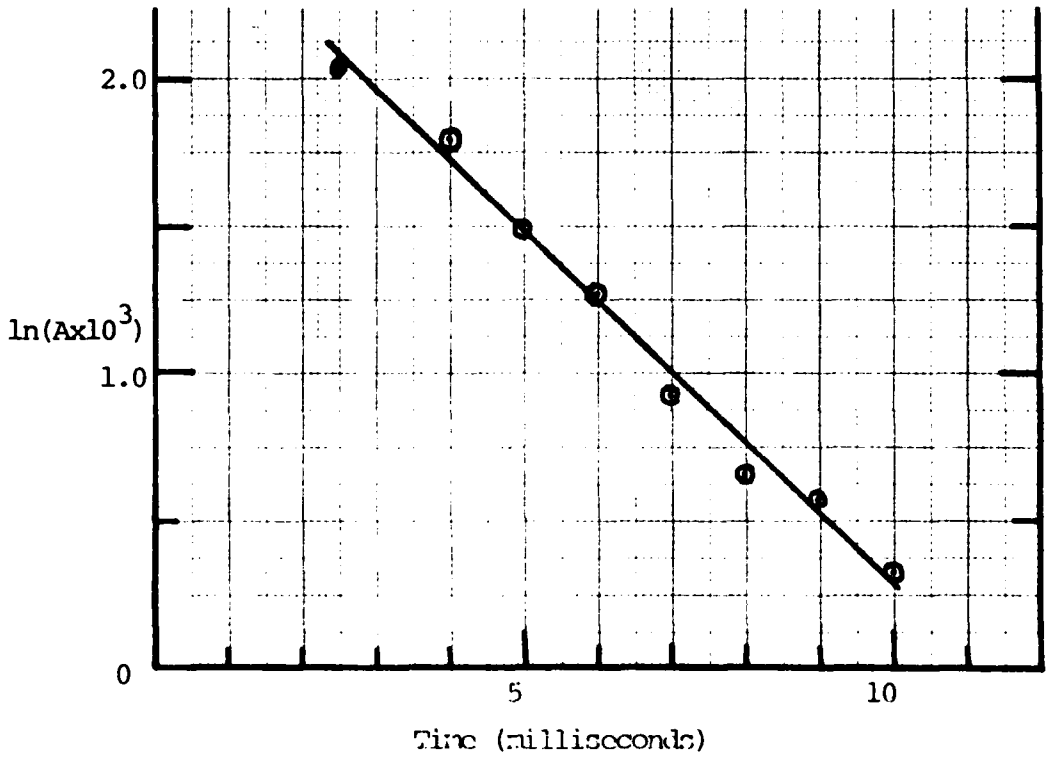

Figure 13. Log Signal Amplitude vs Time: 1.0 torr Ozone

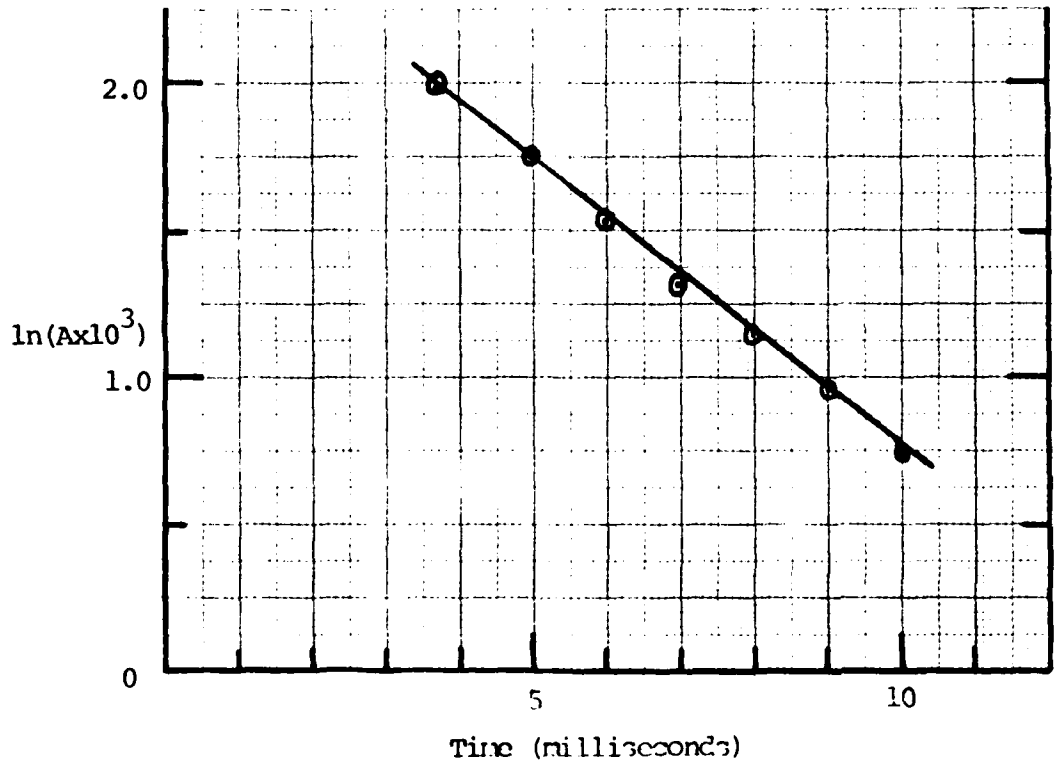

Figure 14. Log Signal Amplitude vs Time: 2.8 torr Ozone

ozone quenching, especially at pressures below 1 torr. Figure 15 is a graph of the data in Table 2. At low concentrations there is a marked difference between the observed and predicted data. This is probably due to $O_2(^1\Delta)$ quenching by trace amounts of iodine contaminating the system. Prior to decay time experiments, an investigation was made into the effect of adding I_2 to the ozone before photolysis. The ozone reacted with the iodine, producing red and yellow streaks and black crystals of iodine residue throughout the iodine mixing vessel and into the photolysis cell. Immediately following the reaction, the ozone pressure dropped from 9 torr to less than 0.1 torr. The iodine trap was replaced and the photolysis cell was cleaned with acetone, then methanol, so that no contamination was visible. However, traces of iodine remained in the stainless steel tubing and, to a lesser extent in the photolysis cell. However, since the contaminated tubing was upstream from the photolysis cell, residual iodine flowed into the cell. Atomic iodine may be produced from residual I_2 by $O_2(^1\Sigma)$ which is a low concentration product of ozone photolysis, by reaction with ozone, or by direct photodissociation of I_2 by the laser pulse. Trace amounts of atomic iodine in the cell would quench $O_2(^1\Delta)$ rapidly.

The quenching of $O_2(^1\Delta)$ by iodine atoms occurs by the following mechanism:

$$O_2(^1\Lambda) + I(^2P_{3/2}) \xrightarrow{k_I} O_2(^3\Sigma) + I^*(^2P_{1/2}) \qquad (30)$$

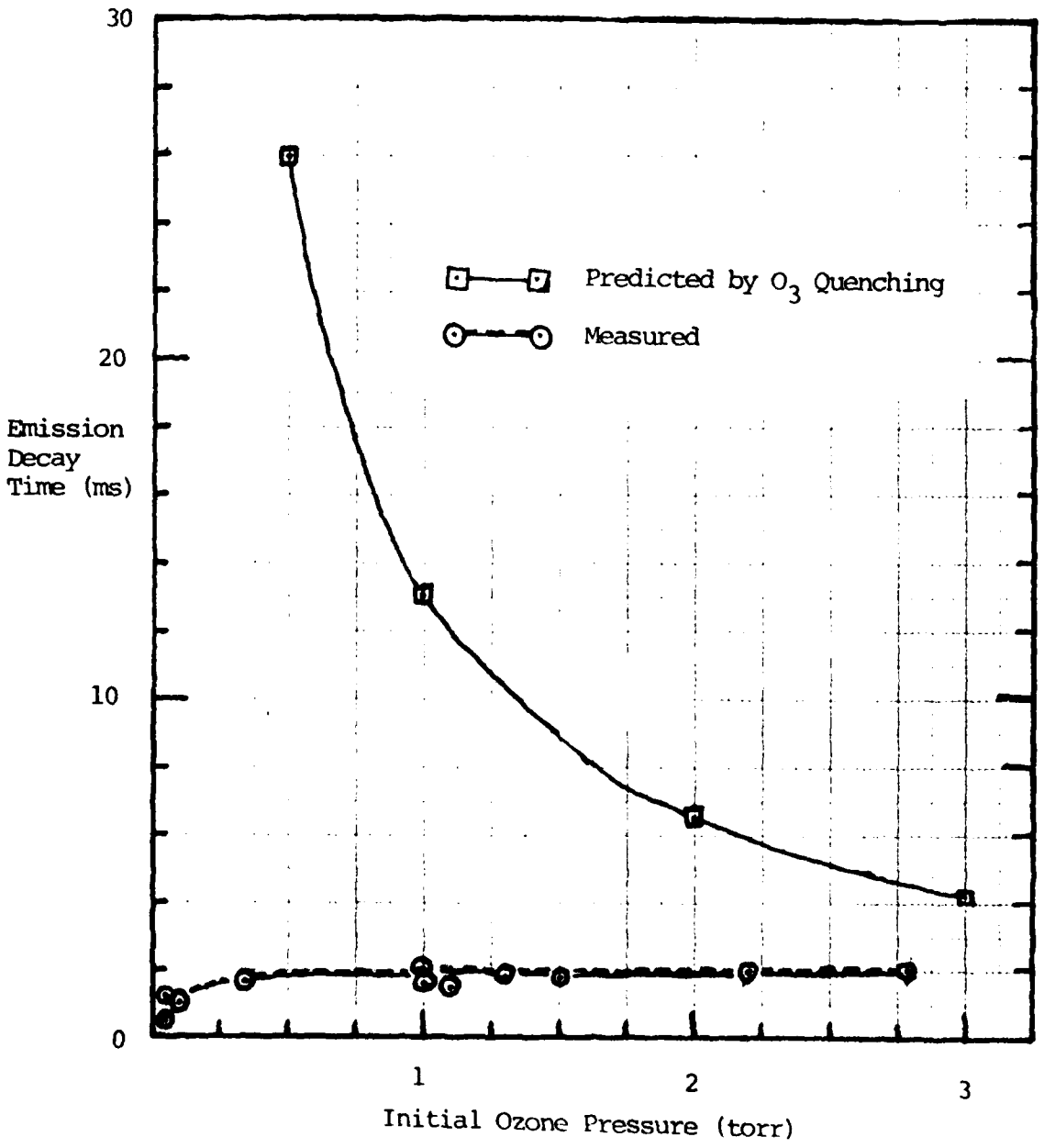

Figure 15. Emission Decay Time vs Initial Ozone Pressure

This is the resonant energy transfer process used in oxygen-iodine lasers. The rate constant, k_I, for reaction (30) is 6.7×10^{-11} cm^3 sec^{-1} (Ref 1:451). Molecular iodine, which is assumed to be present much more abundantly than atomic iodine, quenches I* at a nearly gaskinetic rate (Ref 2:54):

$$I_2 + I^* \xrightarrow{k_{I_2}} I_2 + I \tag{31}$$

Since reaction (31) occurs much more rapidly than reaction (30), the overall rate is limited by the kinetics of reaction (30). The rate expression for reaction 30 is:

$$\text{Rate} = \frac{-d[O_2(^1\Delta)]}{dt} = k_I[O_2(^1\Delta)][I] \tag{32}$$

The characteristic time τ_C of this exponential decay is the initial concentration of $O_2(^1\Delta)$ divided by the initial rate.

$$\tau_C = \frac{[O_2(^1\Delta)]}{k_I[O_2(^1\Delta)][I]} \tag{33}$$

so

$$\tau_C = \frac{1}{k_\tau[T]} \tag{34}$$

This expression is independent of $[O_2(^1\Delta)]$, which agrees well with the data above 1 torr shown in Figure 16. The best horizontal line fit of τ_C to the observed data is the average of the measured characteristic times. This gives

τ_c = 1.81 m sec, and [I] = 7.2 x 10^{12} molecules per cm^3 or 0.21 millitorr of iodine atoms present. This pressure of iodine atoms is reasonable, since the I_2 contamination of the steel tubing was clearly visible.

The amount of light emitted from $O_2(^1\Delta)$ at 6340Å and 1.27μ was less than expected. At a 6340Å monochromator setting, the photomultiplier tube did not detect any radiation. From the appendix, one can see that 1 torr of ozone dissociates to form $O_2(^1\Delta)$ which gives off 1.8 x 10^{-9} watts at 6340Å. From the photomultiplier system data in section 2, this corresponds to a final signal of 17 millivolts, which should have been detected. Thus, if light was produced in the visible, it was shifted away from 6340Å.

At 1.27μ radiation was detected but it was less than the theory predicted. From the appendix, at 1 torr initial ozone pressure, 5.9 x 10^{-9} watts of 1.27μ radiation should be produced. This corresponds to an output from the detector system of 13 volts. The output of the detector, when the interference filter at 1.27μ was removed, was approximately 1 volt. With the filter in place, the detector produced only 7 millivolts. This indicates that less than one percent of the radiation striking the detector was at 1.27μ, and that most of the radiation was outside the bandwidth of the filter.

If $O_2(^1\Delta)$ was produced in an excited vibrational state, the wavelength of light emitted would be shifted from 1.27μ to 1.03μ (Ref 8:560), which is beyond the bandwidth of the

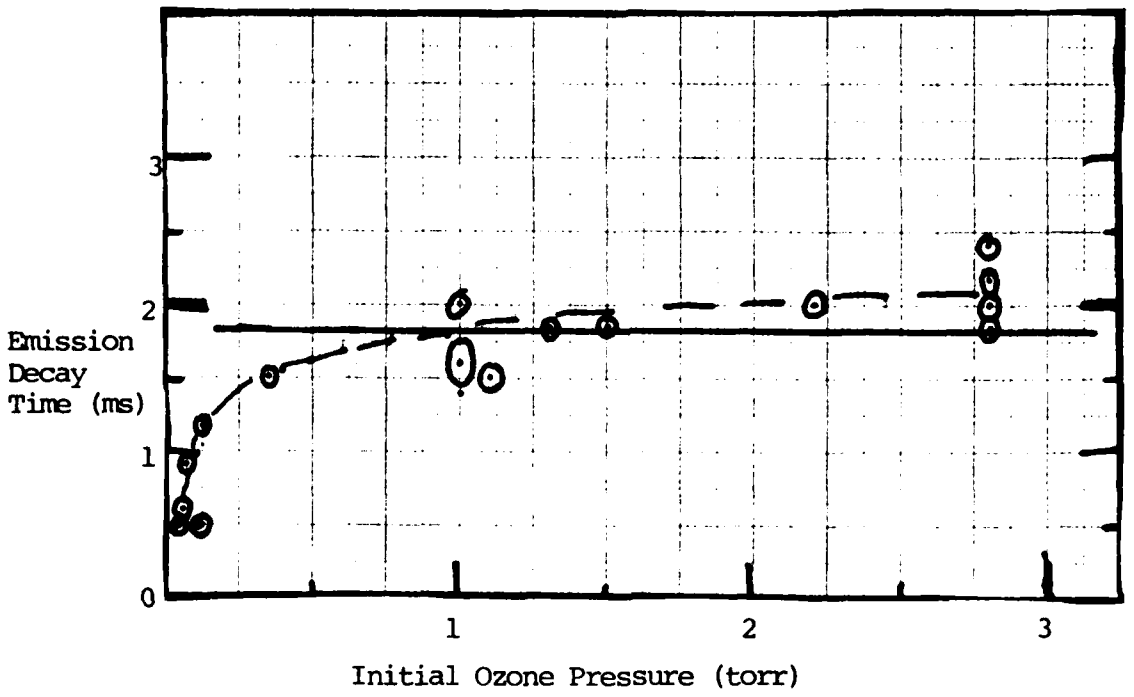

Figure 16. Fit of I* Quenching Hypothesis to Observed Data

filter, but within the 0.8-1.7μ bandwidth of the detector. In a previous experiment, hot band production of $O_2(^1\Delta)$ via uv photolysis of ozone was reported (Ref 9:1402). A frequency quadrupled Nd:YAG laser at 2660Å photolyzed ozone, producing $O_2(^1\Delta)_{v=0}$ (57%), $O_2(^1\Delta)_{v=1}$ (24%), $O_2(^1\Delta)_{v=2}$ (12%), and $O_2(^1\Delta)_{v=3}$ (7%). The present experiment used a laser with shorter wavelength and higher pulse energy, which should produce an increased population of excited vibrational states.

On the other hand, the transition from $O_2(^1\Delta)_{v=0}$ to $O_2(^3\Sigma)_{v=1}$ has been reported at 1.58μ (Ref 15:3). This wavelength is out of the range of the filter but within the detector bandwidth. An analysis of the vibrational states of $O_2(^3\Sigma)$ following ozone photolysis has shown that population of hot bands occurs up to v=21 (Ref 9:1401). This may account for the shift in wavelength observed in the present experiment. A lack of time presented the examination of 1.03μ and 1.58μ emission lines.

To summarize, the quenching time of $O_2(^1\Delta)$ as measured by the decay of 1.27μ emission was less than ozone quenching would predict. An explanation is that traces of iodine quenched $O_2(^1\Delta)$ rapidly. Fitting the theoretical iodine quenching times to the data would give an iodine atom pressure of 0.21 millitorr. Significant population of hot band vibrational states in either $O_2(^1\Delta)$ or $O_2(^1\Sigma)$ may have shifted the wavelength of the transitions in both the visible and the infrared, producing much less light than

anticipated at 6340Å and 1.27μ.

Combustion of Ozone

At 2.8 torr, marked changes occurred in the radiation emitted from the photolysis cell. Emission decay times below 2.8 torr were less than 2 milliseconds. At 2.8 torr, the emission decay time jumped to 3.5 milliseconds. Figure 17 shows this sharp rise. The peak delay time (the lag between laser pulse and emission peak) jumped from 0.5 milliseconds for points below 2.8 torr to greater than 2 milliseconds for points above 2.8 torr. Figure 18 shows the sharp rise in peak delay times. Finally, the amplitude of the detector's signal rose by almost 2 orders of magnitude above 3 torr. The signal amplitude for points below 2.8 torr was 7 2 millivolts (Figures 10-12). Above 3 torr, signal peaks of 450±20 millivolts were produced (See Figure 19). During photolysis at ozone pressures above 3 torr, an orange glow was visible inside the photoylis cell. A spectrograph showed this glow to be a doublet centered at 5860±50Å, with peak separation 10±4Å. No other lines were present in the spectrograms taken from 4800Å to 6500Å. The appearance of the glow coincides with data from the absorption monitoring system which shows ozone is rapidly destroyed. The brighter the glow, the more total was the elimination of ozone. This must be combustion of the ozone. Above 5 torr initial pressure of ozone, complete combustion occurred. The pressure gauge read a constant total gas

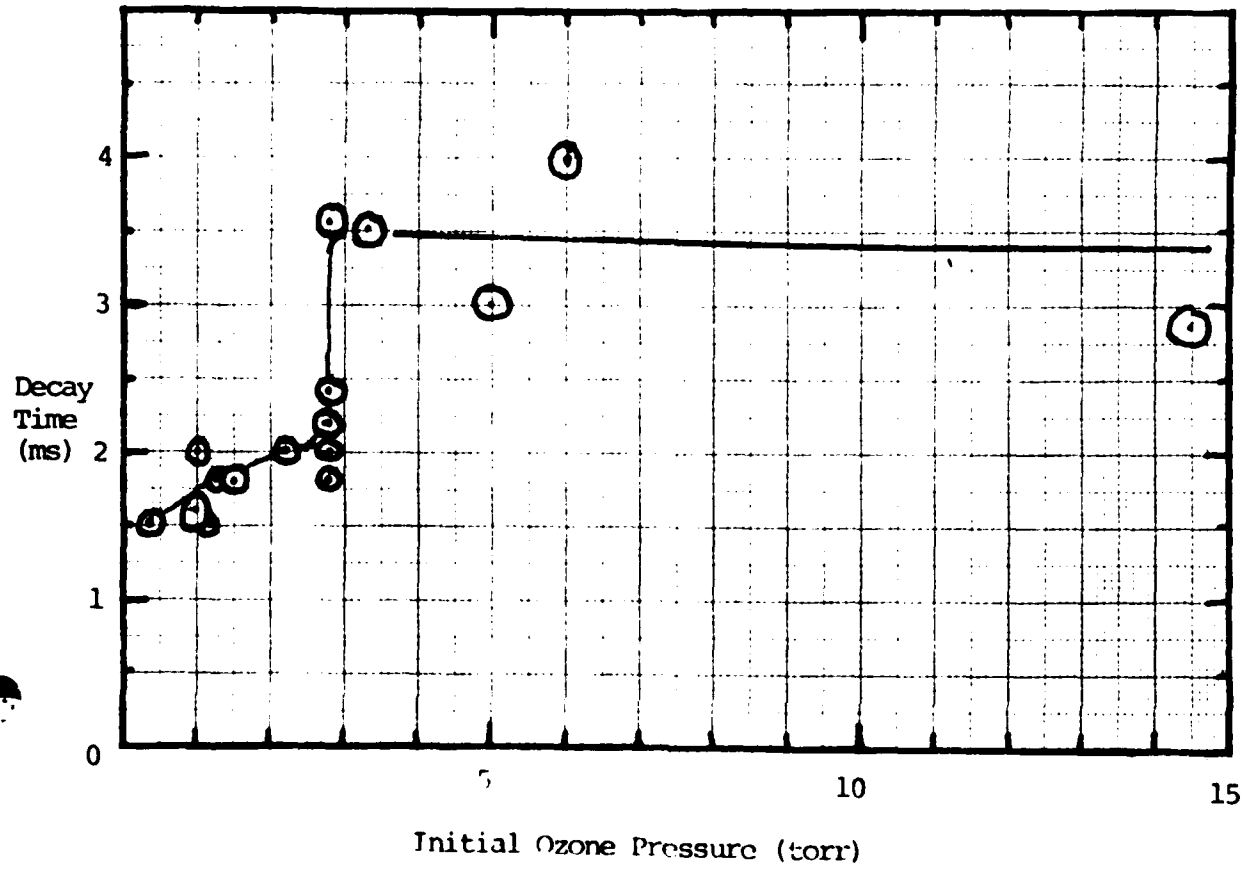

Figure 17. Emission Decay Time vs Initial Ozone Pressure: 0-15 torr

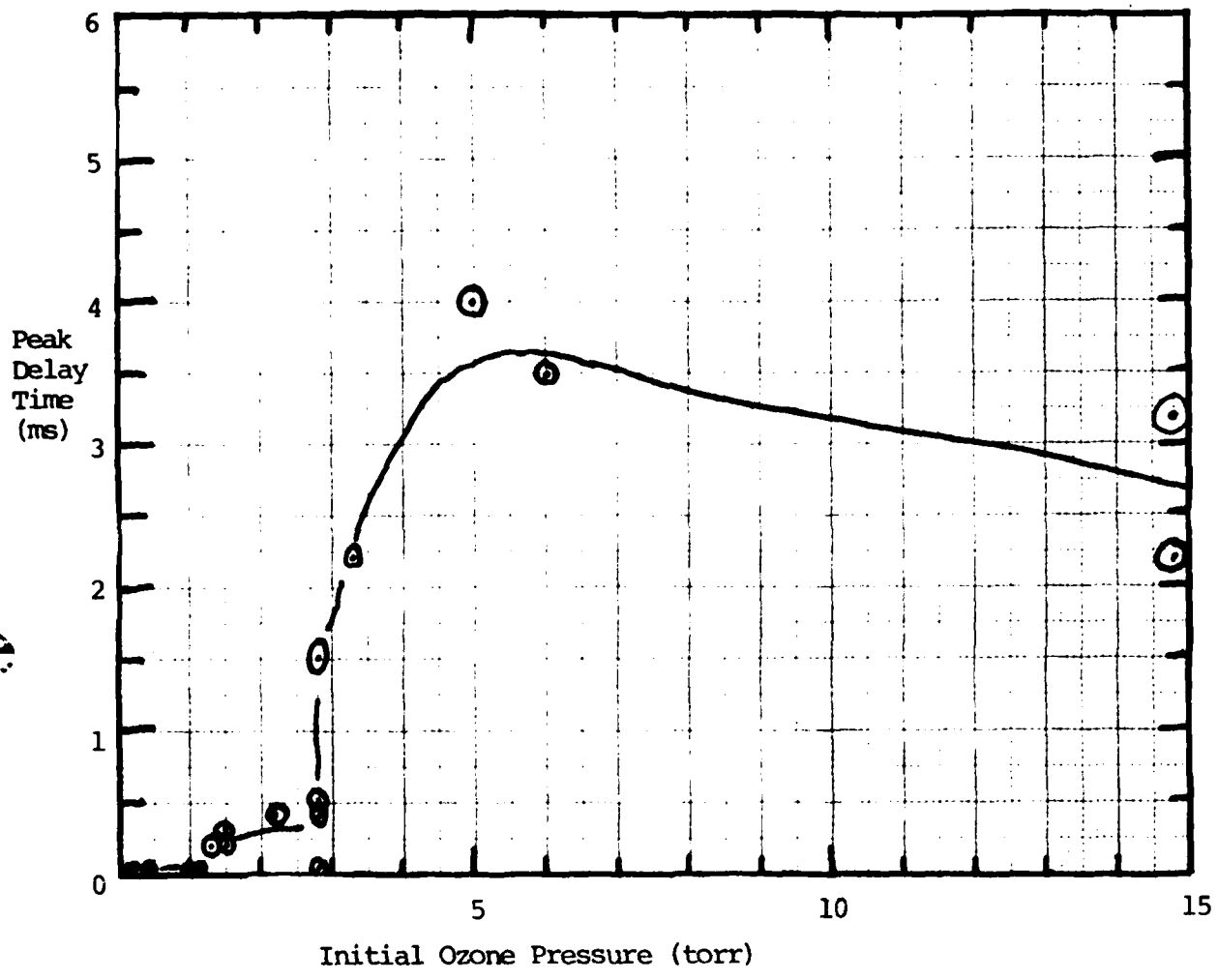

Figure 18. Peak Delay Time vs Initial Ozone Pressure

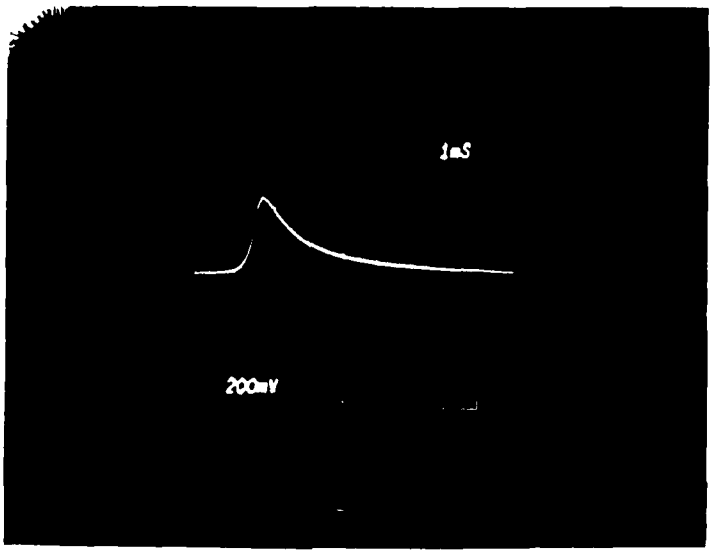

Figure 19. 1.27μ Radiation emitted During Combustion of 15 torr of Ozone

pressure, to within 5%, but the absorption varied from approximately 100% before combustion to 0% after combustion. Mechanisms for combustion of ozone are given in equations (25) to (28).

Combustion of ozone in air at atmospheric pressure has been reported to occur with a blue flame (Ref 14:38). Detonation of ozone-oxygen mixtures at 1 atmosphere in an enclosed shock tube produced a pink glow (Ref 5:34). The orange glow observed in this experiment from ozone combustion at low pressures was not mentioned in the combustion or detonation reports. Nor was it mentioned by researchers using pulsed lasers to dissociate ozone at pressures below 10 millitorr. This is because combustion is visible only above 2.8 torr.

At pressures above 10 torr, an audible "pop" accompanied the brightest laser pulses. The glow extended 3 meters from the photolysis cell back to the silica gel trap, where it was very bright due to the large volume of ozone present. Ozone detonation inside a silica gel trap has been reported (Ref 6:47), but no mention was made of the color of the glow. Following detonation inside the silica gel, several seconds passed with no ozone detected, then the ozone concentration increased to a level higher than the pre-detonation level. The absence of ozone is due to combustion purging the lines of ozone; and the subsequent increased concentration is due to heating of the silica gel by combustion in the trap. The time lag arises because it

takes the ozone several seconds to travel from the silica gel trap to the absorption cell.

An examination of the spectroscopy of the ozone-oxygen system eliminates several potential transitions which might be responsible for the glow seen during combustion. The 5860Å doublet is not due to electronically excited oxygen atoms relaxing to the ground state. The $O^*(^1D) - O(^3P)$ transition occurs at 6300Å in the absence of spin-orbit effects (Ref 4:42). It is also not due to emission from electronically excited ozone molecules. The $\tilde{B}-\tilde{X}$ transition in ozone occurs in a diffuse band from 6100Å to 5500Å (Ref 16:604). Further, it is not due to transitions between different O_2 electronic states with no vibrational excitation. However, the orange glow may be due to electronic transitions in the O_2 spectrum with different vibrational states. A 5800Å line in the emission spectrum of excited oxygen has been observed and assigned to the following transition (Ref 13:658):

$$O_2(^1\Delta)_{v=0} + O_2(^1\Delta)_{v=1} \rightarrow O_2(^3\Sigma)_{v=0} + O_2(^3\Sigma)_{v=0} + h\nu \quad (\lambda=5800\text{Å}) \tag{35}$$

Though this line was reported to be much dimmer than the 6340Å line at room temperatures when $O_2(^1\Delta)$ was produced by microwave discharge, it is expected to be increased in intensity at the ozone combustion temperature, which is 2677°K (Ref 14:38). This transition assignment of the

orange glow observed in this experiment at 5860Å is in agreement with the infrared data mentioned earlier at low pressures, which suggests emission by $O_2(^1\Delta)$ molecules in excited vibrational states.

The time behavior of the emission of 1.27μ radiation during combustion is shown in Figure 20. The 3 millisecond delay in emission after the laser pulse indicates a combustion chain reaction takes place. During the first 3 milliseconds this chain reaction denies the formation and radiation of $O_2(^1\Delta)$. If $O_2(^1\Delta)$ were formed, radiation immediately following the laser pulse would occur, as was seen in Figures 10 and 11. This data suggests that during ozone combustion $O_2(^1\Delta)$ and O* were collisionally deactivated in chain reactions and their energy went to ozone dissociation rather than radiative emission. When the ozone was destroyed (after 3 milliseconds) the radiative emission was stronger and decayed more slowly than in the low pressure, no combustion data. During detonations, the delay in emission may be due to the formation of a shock wave and its reflection from the walls of the photolysis cell. The propagation velocity of ozone detonation shock fronts from initial ozone pressures of 10 torr is extrapolated to be 400 cm/sec (Ref 5:33). The walls of the photolysis cell are 0.5 cm to 2 cm from the center, where the shock starts. Thus, it takes 2.5-10 milliseconds for a shock front to go from center to wall and back. This is approximatey equal to the 3-5 millisecond delays which were

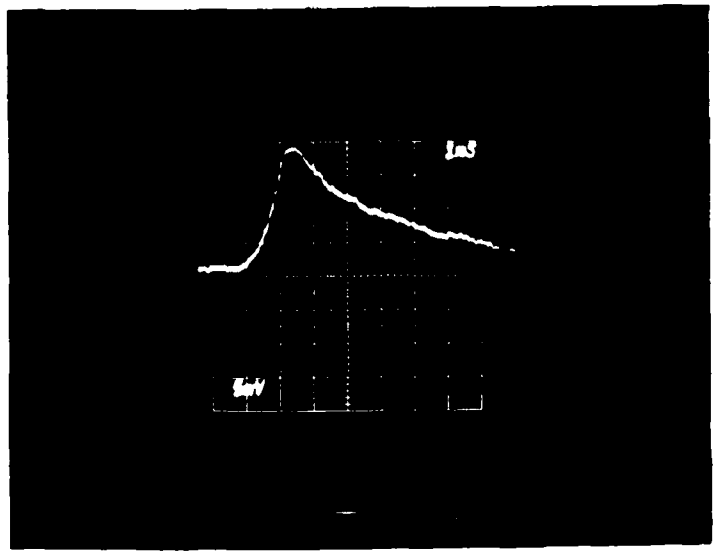

Figure 20. Emission of 1.27μ Radiation During Combustion of Ozone

observed. An audible "pop" indicated shock wave formation during the brightest combustions. The shock wave traveled approximately 3 meters from the photolysis cell to the silica gel in approximately 1 second, which is consistent with a theoretical shock wave velocity of 400 cm/sec.

When helium was flowed with the ozone into the photolysis cell, the peak delay times were reduced by 30% to 2-3 milliseconds. Detonations traveling to the silica gel occurred three times less frequently with helium flowing, but the detonations were stronger. One detonation was strong enough to blow the polyethylene tube from the silica gel trap out of its swagelock connector to a stainless steel tube. The tube end had melted partially closed due to excessive heat from combustions and was blown out of the connector by overpressure from a detonation wave. Since the apparatus was enclosed in a steel-framed box with plexiglass sides, no further damage occurred. Extreme care should be taken in future higher pressure detonation experiments to avoid breaking the glass silica gel trap while it is immersed in the oil bath. When particles of silica gel with ozone adsorbed were dropped into oils at room temperature in a previous experiment, the oils were ignited (Ref 6:47).

In summary, combustion of ozone occurred when ozone at pressures above 3 torr was irradiated with pulses from the excimer laser. The orange glow observed during combustion was a doublet at 5860±50Å. This is consistent with a previous paper which reported a 5800Å line due to the

cooperative emission of $O_2(^1\Delta)_{v=1}$ with $O_2(^1\Delta)_{v=0}$. The combustion was complete when the initial ozone pressure was above 5 torr, and a detonation wave traveled 3 meters back to the silica gel trap when the initial ozone pressure exceeded 10 torr. The detonation shock produced an audible "pop" and traveled at approximately the reported detonation wave velocity of 400 cm per second. The addition of helium to the ozone flow decreased the rate of detonations, but increased their intensity.

V. Recommendations

To determine the processes which occur when ozone at pressures between 0.1 torr and 20 torr is photolyzed by a pulsed uv laser, the emission wavelengths must be measured. The present experiment found that emission is not as expected at 6340Å and 1.27μ. Either the infrared spectrum of the emission should be measured, or the level of emission at 1.03μ and 1.58μ should be measured. The wavelength of the observed orange glow at 5860±50Å should be measured accurately using a photomultiplier tube and tuning spectrometer. The minimum ozone pressure which produces detectable light at this wavelength should be determined. Since ozone combustions could rupture the glass silica gel trap, and since ozone-impregnated silica gel pellets dropped in oil ignite the oil, the oil bath should not be placed around the trap during combustion measurements.

In order to use laser-induced ozone photolysis for $O_2(^1\Delta)$ production in high energy oxygen-iodine lasers, several problems must be overcome. First, the excitation of upper vibrational states must be eliminated. This could be accomplished by adding a species which absorbs energy at the wavelength caused by the hot band transition. Since the oxygen-iodine system depends on resonant energy transfer to the iodine atom's excited state at 1.315μ, vibrational deviations of 0.2μ from the 1.27μ $O_2(^1\Delta)_{v=0}$ state cannot be tolerated. The infrared spectrum of the photolysis products

emission should be examined to determine which excited vibrational and electronic states occur. Although the concentration of $O_2(^1\Sigma)$ produced by ozone photolysis is projected to be negligible due to rapid ozone quenching (Ref 1:452, 455) its 7680Å emission band should be examined. Second, the problem of ozone combustion must be overcome. This may be accomplished by decreasing the laser intensity with a beam expander or by installing a flame retarding screen inside the photolysis cell.

To scale up the process of pulsed laser photolysis of ozone, several factors should be investigated. Higher pulse repetition rates will reduce the amount of undissociated ozone. Mirrored walls of the photolysis cell would allow each pulse to pass several times through the ozone, increasing the efficiency. Such a mirrored cell has previously been used for ozone dissociation (Ref 4:40). Finally, increasing the size of the cell could increase the molar flow rate while keeping the pressure below the 3 torr combustion threshold. This would raise the amount of $O_2(^1\Delta)$ produced. If the problems of ozone detonation and hot band excitation are overcome, laser photolysis of ozone may be scaled to compete with the widely used chemical process of $O_2(^1\Delta)$ formation for use in high energy oxygen-iodine lasers.

Bibliography

1. Didyukov. A.I., Y.I. Krasnoshchekov, Y.A. Kulagin, V.A. Morozov, S.A. Reshetnyak, and L.A. Shelepin. "Photolytic Generator of Excited Oxygen $O_2(a^1\Delta g)$," Soviet Journal of Quantum Electronics, 12 (4): 451-455 (April 1982).

2. Heidner, R.F., J.G. Coffer, and C.E. Gardner. "$O_2(^1\Delta)$-I Atom Energy Transfer Studies: CW Inversion on 1.315- m I-Atom Transition," SAMSO TR-77-215 Interim Report. El Segundo, California: Aerospace Laboratory, The Ivan A. Getting Laboratories, The Aerospace Corporation, 15 December 1977.

3. Gauthier, M. and D.R. Snelling. "Mechanism of Singlet Molecular Oxygen Formation from Photolysis of Ozone at 2537Å," Journal of Chemical Physics 54 (10): 4317-4325 (15 May 1971).

4. Amimoto, S.T., A.P. Force, and J.R. Wiesenfeld. "Ozone Photochemistry: Production and Deactivation of $O(2^1D_2)$ Following Photolysis of Ozone at 248 nm," Chemical Physics Letters 60 (1): 40-43 (15 December 1978).

5. Harper, S.A. and W.E. Gordon. "Detonation Properties of Ozone," Ozone Chemistry and Technology. Washington, D.C.: American Chemical Society, March 1959.

6. Cook, G.A., A.D. Kiffer, C.V. Klumpp, A.H. Malik, and L.A. Spence. "Separation of Ozone from Oxygen by a Sorption Process," Ozone Chemistry and Technology. Washington, D.C.: American Chemical Society, March 1959.

7. McDermott, W.E., N.R. Pchelkin, D.J. Benard, and R.R. Bousek. "An Electronic Transition Chemical Laser," Applied Physics Letters 32 (8): 469-470 (15 April 1978).

8. Herzberg, Gerhard. Molecular Spectra and Molecular Structure I. Spectra of Diatomic Molecules (Second Edition). Princeton, New Jersey: D. Van Nostrand Company, 1950.

9. Sparks, R.K., L.R. Carlson, K. Shobatake, M.L. Kowalczyk, and Y.T. Lee. "Ozone Photolysis: A Determination of the Electronic and Vibrational State Distributions of Primary Products," Journal of Chemical Physics 72 (2): 1401-1402 (15 January 1980).

10. Griggs, M. "Absorption Coefficients of Ozone in the Ultraviolet and Visible Regions," Journal of Chemical Physics 49: 857 (1968).

11. Collins, R.J., D. Husain, and R.J. Donovan. "Kinetic and Spectroscopic Studies of $O_2(a^1\Delta g)$ by Time-Resolved Absorption Spectroscopy in the Vacuum Ultraviolet," Journal of the Chemical Society Faraday Transactions II 69: 145-157 (1973).

12. Clark, J.D. and R.P. Wayne. "The Collisional Deactivation of $O_2(^1\Delta g)$," Chemical Physics Letters 3 (2): 93-95 (February 1969).

13. Gray, E.W. and E.A. Ogryzlo. "The Cooperative Emission Bands of 'Singlet' Molecular Oxygen," Chemical Physics Letters 3 (9): 658-660 (1 September 1969).

14. Streng, A.G. and A.V. Grosse. "Pure Ozone Flame and the Combustion of Various Fuel Gases in Pure Ozone," Ozone Chemistry and Technology. Washington, D.C. American Chemical Society, March 1959.

15. ADC Product Specification. "I-R Detector Systems Model 403," Fresno, California: Applied Detector Corporation, January 1978.

16. Herzberg, Gerhard. Molecular Spectra and Molecular Structure III: Electronic Spectra of Polyatomic Molecules. New York: Van Nostrand Reinhold Company, 1966.

Appendix: Calculations of Expected Concentration, Quenching, and Emission of $O_2(^1\Delta)$

If an initial pressure of ozone is assumed to be 1 torr, equation (10) shows that after a 16 nanosecond laser pulse, 0.39 torr of ozone remains, and 0.61 torr of has been dissociated. Equation (10) was obtained by assuming the laser intensity to be uniform throughout the photolysis region. However, the absorption of laser light by ozone in the cell attenuates the laser pulse as it penetrates deeper into the ozone. The attenuation of intensity follows the Beer-Lambert law:

$$I = I_0 e^{-\alpha \ell} \qquad \text{(A-1)}$$

where α is the absorption coefficient

ℓ is the distance penetrated

For ozone, α is 131 cm^{-1} atm^{-1} (Ref 10:857), so for 1 torr α is $0.17 cm^{-1}$. Figure A-1 shows the variation of intensity with penetration depth. After the pulse penetrates to the end of the 4 cm cell its intensity drops to 51% of the original intensity. The rate of dissociation (and hence the amount of ozone dissociated) at each depth is proportional to the intensity of light at that depth. The total amount of ozone dissociated is proportional to the area under the intensity curve, which is 73.5% of the area under the square

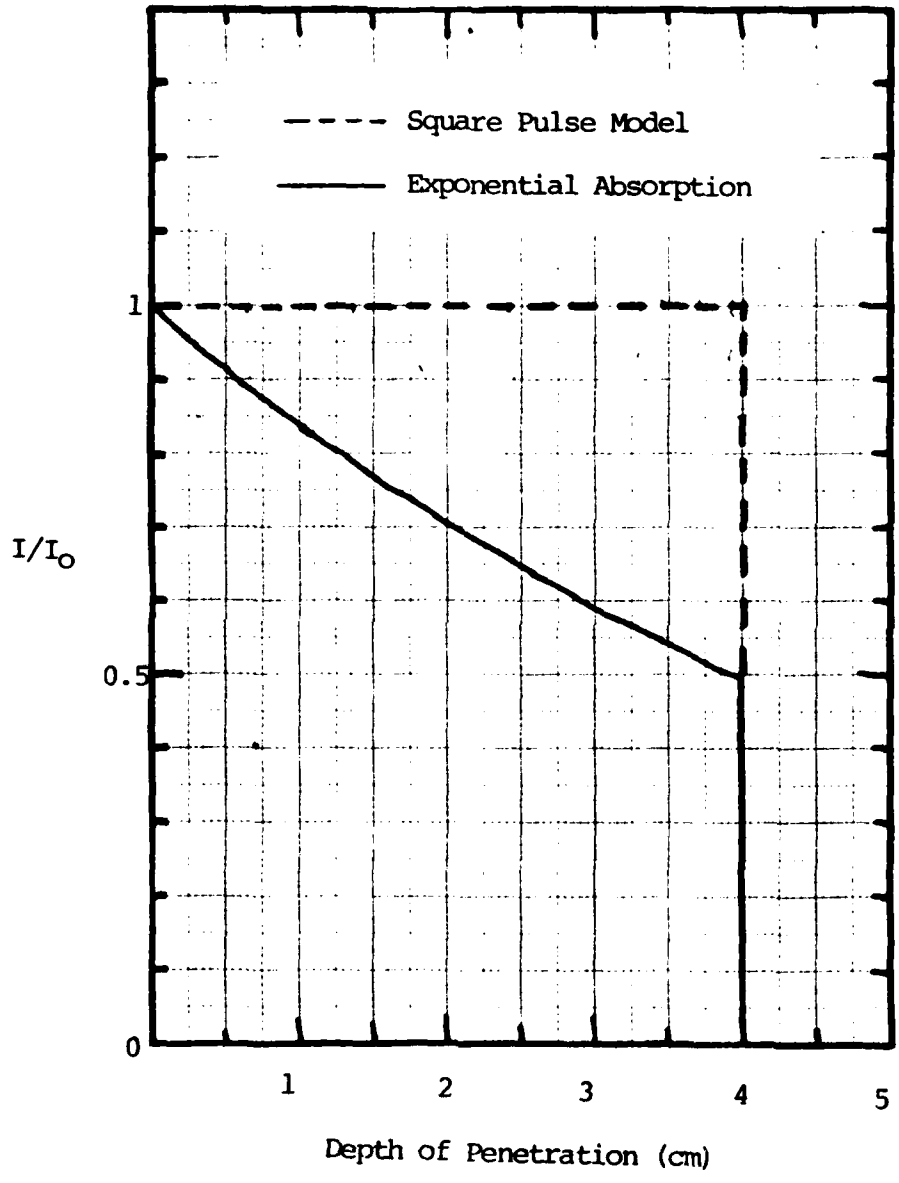

Figure A-1. Variation of Laser Pulse Intensity With Depth of Penetration

pulse assumed curve. Thus the actual amount of ozone dissociated is 73.5% of 0.61 torr, or 0.45 torr. This means that 0.45 torr of O_2 is produced, rather than the originally estimated 0.61 torr. Approximately 90%, or 0.4 torr of the oxygen is $O_2(^1\Delta)$.

The quenching of 0.4 torr of $O_2(^1\Delta)$ by the 0.55 torr of ozone which has not dissociated occurs as follows. From Table 1, the rate constant for ozone quenching of $O_2(^1\Delta)$ is 4×10^{-15} $cm^3\,sec^{-1}$. Ozone at a pressure of 0.55 torr corresponds to 1.9×10^{16} ozone molecules per cubic centimeter. Thus the rate of quenching is 77 sec^{-1} and the characteristic time of the quenching reaction is 13 milliseconds. The characteristic time for quenching by ground state oxygen $O_2(^3\Sigma)$ is found as follows. Of 0.45 torr total oxygen produced by photolysis, 10% or 0.045 torr is $O_2(^3\Sigma)$. This corresponds to 1.5×10^{15} $O_2(^3\Sigma)$ molecules per cubic centimeter. The rate constant for $O_2(^1\Delta)$ quenching of $O_2(^1\Delta)$ is 2×10^{-18} $cm^3\,sec^{-1}$. This gives a quenching rate of 3×10^{-3} sec^{-1}, which is 4 orders of magnitude slower than the ozone quenching rate. All other anticipated quenching rates are at least 3 orders of magnitude slower than the ozone quenching rate, so they can be neglected. Ozone is projected to be the dominant quenching agent.

The radiative emission of a 1.27μ photon from $O_2(^1\Delta)$ occurs with a characteristic time τ_r of 3.6×10^3 seconds. According to equation (20), the number of photons emitted

per second is approximately N_0/τ_r. N_0 is the number of $O_2(^1\Delta)$ molecules present. Assuming a 1 cm^3 photolysis region (0.25 cm^2 beam traversing a 4 cm cell), and 0.4 torr of $O_2(^1\Delta)$ in that region, N_0 becomes 1.4×10^{16} molecules. Thus there are 3.8×10^{12} photons per second emitted at 1.27μ. Each photon has an energy of:

$$\frac{hc}{\lambda} = 1.56 \times 10^{-19} \text{ J} \qquad \text{(A-2)}$$

So the power emitted is the number of photons per second times the photon energy, or 5.9×10^{-7} watts at 1.27μ.

The cooperative emission of a 6340Å photon by two $O_2(^1\Delta)$ molecules has a rate constant of 3×10^{-23} cm^3 sec^{-1}. If 0.4 torr of $O_2(^1\Delta)$ is present, the rate of emission is 4.2×10^{-7} sec^{-1}, giving a characteristic time τ_r or 2.4×10^6 sec. Thus 5.8×10^9 photons per second are emitted at 6340Å, which corresponds to a power of 1.8×10^{-9} watts. This is more than two orders of magnitude lower than the power at 1.27μ.

Vita

Captain Lee Paul Schelonka was born on 19 May 1957 in Milwaukee, Wisconsin. He graduated from high school in Satellite Beach, Florida in 1974. He attended the University of Colorado under a four-year Air Force ROTC scholarship and received a Bachelor of Arts degree in Physics in 1978. Upon graduation he received a commission in the United States Air Force and was assigned to the Inertial Guidance Laboratory of the 6585th Test Group at Holloman Air Force Base. While there, he developed the astronomic references for testing the MX missile inertial guidance system. During off-duty hours, he enrolled in a Masters degree program in International Relations through New Mexico State University and received a Master of Science degree in 1982. He entered the School of Engineering, Air Force Institute of Technology, in June 1982.

Unclassified
SECURITY CLASSIFICATION OF THIS PAGE

REPORT DOCUMENTATION PAGE

1a. REPORT SECURITY CLASSIFICATION Unclassified	1b. RESTRICTIVE MARKINGS
2a. SECURITY CLASSIFICATION AUTHORITY	3. DISTRIBUTION/AVAILABILITY OF REPORT Approved for public release; distribution unlimited.
2b. DECLASSIFICATION/DOWNGRADING SCHEDULE	
4. PERFORMING ORGANIZATION REPORT NUMBER(S) AFIT/GEP/PH/83D-12	5. MONITORING ORGANIZATION REPORT NUMBER(S)
6a. NAME OF PERFORMING ORGANIZATION School of Engineering AF Institute of Technology 6b. OFFICE SYMBOL (If applicable) AFIT/EN	7a. NAME OF MONITORING ORGANIZATION
6c. ADDRESS (City, State and ZIP Code) Wright-Patterson AFB, OH 45433	7b. ADDRESS (City, State and ZIP Code)
8a. NAME OF FUNDING/SPONSORING ORGANIZATION AF Weapons Laboratory 8b. OFFICE SYMBOL (If applicable) ARAY	9. PROCUREMENT INSTRUMENT IDENTIFICATION NUMBER
8c. ADDRESS (City, State and ZIP Code) Kirtland AFB, NM 87117	10. SOURCE OF FUNDING NOS. PROGRAM ELEMENT NO. / PROJECT NO. / TASK NO. / WORK UNIT NO.
11. TITLE (Include Security Classification) Pulsed Generation of Singlet Delta Oxygen Via Ozone Photolysis	
12. PERSONAL AUTHOR(S) Lee Paul Schelonka, Capt, USAF	
13a. TYPE OF REPORT MS Thesis 13b. TIME COVERED FROM _____ TO _____	14. DATE OF REPORT (Yr., Mo., Day) 1983, December 15. PAGE COUNT 66
16. SUPPLEMENTARY NOTATION	Lynn Wolaver 7 Feb 84 Dean for Research and Professional Development Air Force Institute of Technology (ATC) Wright-Patterson AFB, OH 45433

17. COSATI CODES		
FIELD	GROUP	SUB. GR.
20	5	
7	5	

18. SUBJECT TERMS (Continue on reverse if necessary and identify by block number)
ozone, oxygen compounds, photolysis, oxygen generators, emission, spectroscopy, pulsed lasers, chemical lasers.

19. ABSTRACT (Continue on reverse if necessary and identify by block number)

Ozone was stored on silica gel at 77°C and photolyzed at pressures from 0.1 torr to 20 torr using an excimer laser of wavelength 2480Å. The wavelength of the emission which was detected following photolysis is in agreement with previously reported "hot band" production of $O_2(^1\Delta)_{v=1}$. Quenching of the emission occurred in 0.5 to 2 milliseconds, which may have been due to resonant transfer from $O_2(^1\Delta)$ to $I(^2P_{1/2})$. The iodine in the system was residual from prior experiments. At pressures above 3 torr, ozone combustions and detonations occurred. Combustion produced an orange glow at 5860±50Å, and detonation produced an audible shock wave which traveled at 4 ± 2 meters per second.

20. DISTRIBUTION/AVAILABILITY OF ABSTRACT UNCLASSIFIED/UNLIMITED ☒ SAME AS RPT. ☐ DTIC USERS ☐	21. ABSTRACT SECURITY CLASSIFICATION Unclassified
22a. NAME OF RESPONSIBLE INDIVIDUAL Ernest A. Dorko, PhD	22b. TELEPHONE NUMBER (Include Area Code) (513) 255-2012 22c. OFFICE SYMBOL AFIT/ENP

DD FORM 1473, 83 APR EDITION OF 1 JAN 73 IS OBSOLETE.

Unclassified
SECURITY CLASSIFICATION OF THIS PAGE

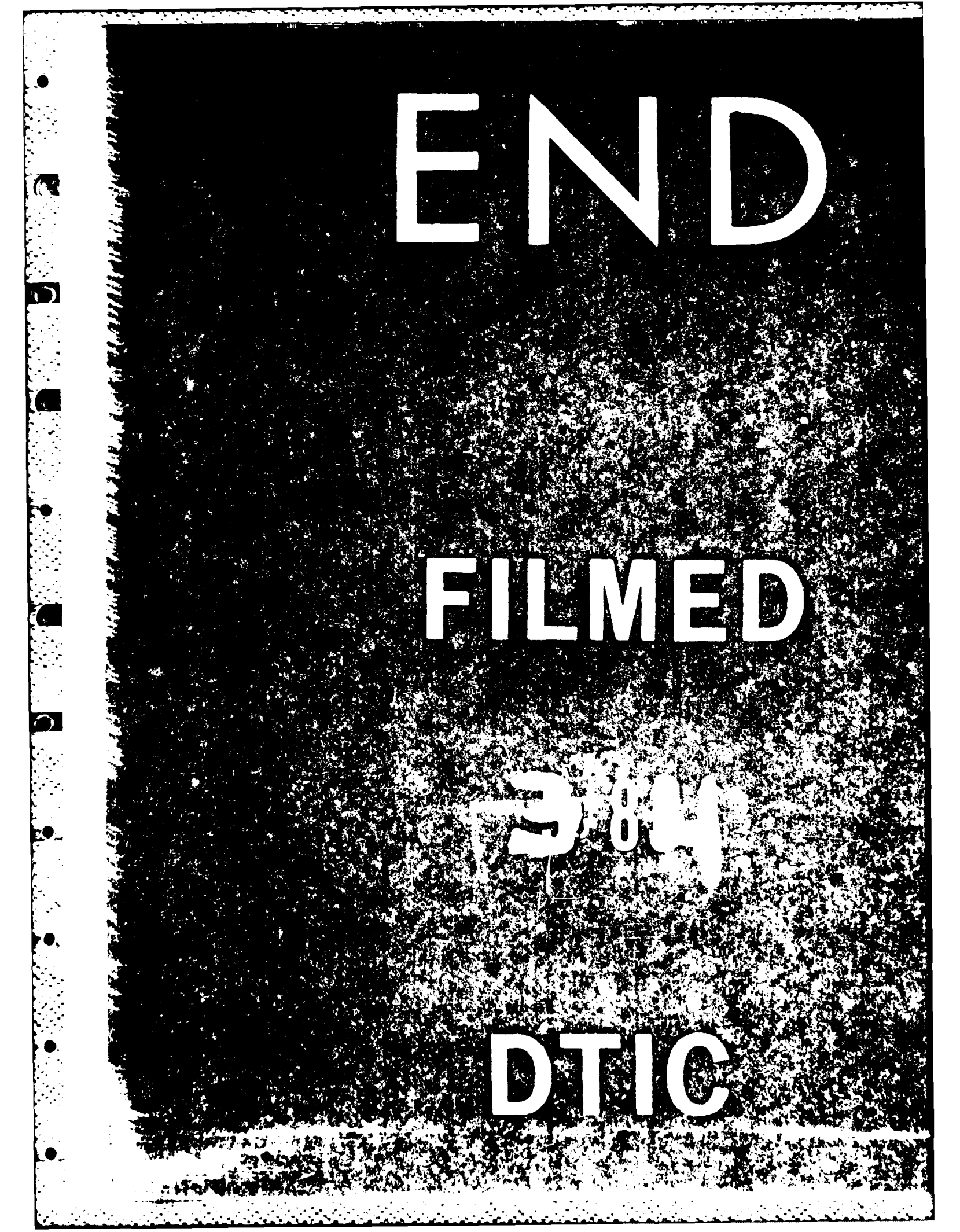
END
FILMED
DTIC